NASA RESEARCH ANNOUNCEMENT

PROPOSAL INFORMATION PACKAGE

Mars Exploration Program
2001 Mars Odyssey Orbiter

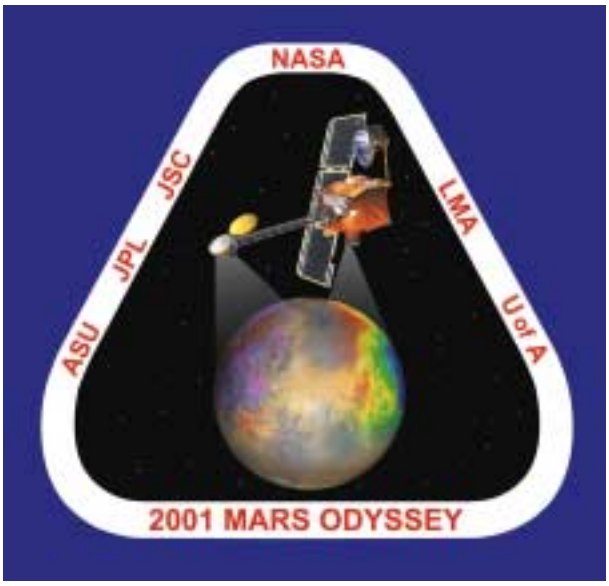

23 July 2001

Contributors

Raymond Arvidson[1]
Gautam Badhwar[2]
William Boynton[3]
Philip Christensen[4]
Jeffrey J. Plaut[5]
Susan Slavney[1]
David A. Spencer[5]

Compiled by

Thomas W. Thompson[5]
Jeffrey J. Plaut[5]
Catherine M. Weitz[6]

[1]Washington University, [2]Johnson Space Center, [3]Lunar and Planetary Laboratory (University of Arizona),
[4]Arizona State University, [5]Jet Propulsion Laboratory, California Institute of Technology [6]NASA Headquarters.

Table of Contents

1.0 Overview 1-1
1.1 Document Overview 1-1
1.2 Mars Exploration Program 1-1
1.3 Mars 2001 Objectives 1-2
1.4 Mars 2001 Operations Management 1-2
1.5 Mars 2001 Orbiter Measurement Synergies through Coordinated Operations Planning 1-2
1.6 Mars 2001 Project Science Group (PSG) Members 1-3

2.0 Mars 2001 Orbiter Operations 2-1
2.1 Science Instruments 2-1
2.1.1 Thermal Emission Imaging System (THEMIS) 2-1
2.1.2 Gamma Ray Spectrometer (GRS) 2-2
2.1.3 Martian Radiation Environment Experiment (MARIE) 2-2
2.2 Initial Science Orbit 2-2
2.3 Orbit Evolution 2-3

3.0 Gamma Ray Spectrometer (GRS) 3-1
3.1 GRS Instrumentation 3-1
3.1.1 Gamma Ray Detector 3-2
3.1.2 Anticoincidence Shield/Neutron Detector 3-3
3.1.3 Radiative Cooler 3-3
3.1.4 The Central Electronics Assembly (CEA) 3-4
3.2 Mission Design and Data Analysis 3-4
3.2.1 Mission Design 3-4
3.2.2 Data Analysis 3-5
3.2.3 Spatial Resolution and Sensitivities 3-6
3.2.4 Reduction of GRS Neutron Data 3-9

4.0 Thermal Emission Imaging System (THEMIS) 4-1
4.1 Scientific Objectives 4-1
4.2 THEMIS Baseline Design 4-1
4.2.1 Infrared Subsystem (IRS) 4-1
4.2.2 Visible Imaging Subsystem (VIS) 4-2
4.2.3 Optical Subsystem 4-3
4.2.4 In-Band Spectral Response 4-3
4.2.5 Out-of-Band Spectral Response 4-3
4.2.6 Spectral Sensitivity 4-3
4.2.7 Instantaneous Field of View (IFOV) 4-4
4.2.8 Ground Sampling Distance (GSD) 4-4
4.2.9 Field of View (FOV) 4-4
4.2.10 Total Encircled Energy 4-4
4.2.11 Modulation Transfer Function (MTF) 4-4
4.2.12 Dynamic Range 4-4
4.2.13 Linearity 4-4
4.2.14 Transient Response 4-4
4.3 VIS Performance 4-5
4.3.1 In-Band Spectral Response 4-5
4.3.2 Out-of-Band Spectral Response 4-5
4.3.3 Spectral Sensitivity 4-5
4.3.4 Instantaneous Field of View (IFOV) 4-5
4.3.5 Ground Sampling Distance (GSD) 4-5
4.3.6 Field of View (FOV) 4-6

4.3.7 Total Encircled Energy 4-6
4.3.8 Modulation Transfer Function (MTF) 4-6
4.3.9 Dynamic Range 4-6
4.3.10 Linearity 4-6
4.4 IRS and VIS Sensor Co-Registration 4-6
4.5 Pointing and Alignment 4-6

5.0 Martian Radiation Environment Experiment (MARIE) 5-1
5.1 Orbiter Instrumentation 5-1

6.0 Additional Information 6-1
6.1 Web Sites 6-1

7.0 References 7-1

8.0 Acronyms 8-1

Appendix A: 2001 Mars Odyssey Orbiter Archive, Generation, Validation, and Transfer Plan A-1

List of Figures

2-1 Orbiter Science Instruments 2-1
2-2 Science Orbit Evolution 2-4
3-1 The Mars Gamma Ray Spectrometer (GRS) 3-1
3-2 The Gamma Ray Spectrometer Sensor Head 3-2
3-3 Calculated Gamma Ray Spectrum from Mars 3-5
3-4 A Portion of the Simulated Spectrum for Mars with Two Different Accumulation Times 3-9
3-5 Energy Flux Spectrum of the $^{10}B(n,\alpha)^{7}$ Li Neutron Capture Reaction in Each Trapezoid of the Anticoincidence Shield/Neutron Detector 3-10
3-6 Contours of the Neutron Response Functions of the Four Individual Faces of the Gamma Ray Spectrometer Anticoincidence Shield/Neutron Detector Subsystem Relative to the Subsatellite Point 3-11
3-7 A Summary of the Correlation Given by Equation (3) 3-12
5-1 Schematic of Orbiter Spectrometer 5-2
5-2 Energy Loss in A1 Detectors vs. Energy Loss in A2 Detectors 5-3

List of Tables

1-1 Mars 2001 Payloads 1-2
2-1 Orbital Characteristics at Completion of Aerobraking 2-3
2-2 Orbiter Science Data Volume Comparison 2-4
3-1 Accumulation Times for the Mars Observer Gamma Ray Spectrometer for One Spatial Resolution Element 3-7
3-2 Accumulation Time at Mars for 10% Relative Uncertainty in Concentration 3-7
3-3 Uncertainty in the Concentration at Mars for Two Accumulation Times 3-8
4-1 THEMIS Infrared Band Characteristics 4-3
4-2 THEMIS Infrared Band Signal-to-Noise Ratio 4-4
4-3 IRS Total Encircled Energy 4-4
4-4 THEMIS Visible Band Characteristics 4-5
4-5 VIS Spectral Sensitivity 4-5
4-6 VIS Total Encircled Energy 4-6

1.0 OVERVIEW

1.1 Document Overview

This Proposal Information Package (PIP) document describes the Mars Exploration Program 2001 Mars Odyssey Orbiter (Mars 2001), in support of the announcement of opportunity for participating scientists (Research Opportunities In Space Science—2001, NRA-01-OSS-01). Section 1.0 is an overview of the Mars Exploration Program and the Mars 2001 mission. Section 2.0 provides an overview of orbiter operations followed by detailed descriptions of the Orbiter instruments: the Gamma Ray Spectrometer (GRS) in Section 3.0, the Thermal Emission Imaging System (THEMIS) in Section 4.0, and the Martian Radiation Environment Experiment (MARIE) in Section 5.0. Section 6.0 provides listing of web sites. Section 7.0 lists the references, and Section 8.0 lists the acronyms used in this document. Appendix A contains a draft of the 2001 Mars Odyssey Orbiter Archive Generation, Validation, and Transfer Plan.

Questions about material in this Proposal Information Package should be submitted in writing to:

Jeffrey Plaut Mars 2001 Deputy Project Scientist
Mail Stop 183-501
Jet Propulsion Laboratory
4800 Oak Grove Drive
Pasadena, CA 91109, USA
Voice: (818) 393-3799 / FAX: (818) 354-0966
e-mail: plaut@jpl.nasa.gov

Replies will be returned in writing. Also, these questions and answers will be posted on the Proposal Information Package Web Site.

1.2 Mars Exploration Program

The National Aeronautics and Space Administration (NASA) has initiated a long-term systematic program of Mars exploration, the Mars Exploration Program (MEP). The highest priority scientific objectives of this program are to:

- search for evidence of past or present life,
- understand the climate and volatile history of Mars, and
- assess the nature and inventory of resources on Mars.

The common thread of these objectives is water: past and present sources and sinks; exchanges between subsurface, surface, and atmospheric reservoirs; and the change of volatiles over time. The goal of the MEP is to carry out low-cost missions, each of which provides important, focused scientific return, and which will in sum constitute a major element of the scientific exploration of Mars. A series of lander and/or orbiter spacecraft are being launched at each favorable Mars launch opportunity, approximately every 26 months. In 1997, the MEP launched the Mars Global Surveyor (MGS), which together with the launch of the Discovery Program's Mars Pathfinder Lander, initiated the new era of Mars exploration. In the 1998–1999 launch opportunity, the MEP launched the Mars Climate Orbiter (which failed to reach Mars orbit) and the Mars Polar Lander (which failed during its landing sequence). Mars 2001 originally consisted of an orbiter and lander, both of which were scheduled for launch in the spring of 2001. However, based upon the recommendations of the Young Report and NASA management, it was decided to delay the launch of the Mars 2001 lander. Therefore, the focus of the 2001 element of the MEP will be to map the elemental and mineralogical composition of the surface via the orbiter instruments.

The Mars 2001 orbiter will carry instruments that will determine surface mineralogy and morphology, provide global gamma ray observations for a full Martian year, and study the Mars radiation environment from orbit. In addition, the orbiter spacecraft will serve as a data relay for future landers. The orbiter science mission extends for 917 days. During the science mission, the orbiter will also serve as a communications relay for U.S. or international

landers in 2003–2004. The orbiter will continue to serve as a telecommunications asset following the science mission; this relay-only phase extends for 457 days, for a total mission duration of 1374 days, or two Mars years. As a goal, an additional Mars year of relay operations is planned.

1.3 Mars 2001 Objectives

The science objectives of the Mars 2001 mission are to:

(1) globally map the elemental composition of the surface,
(2) determine the abundance of hydrogen in the shallow subsurface,
(3) acquire high spatial and spectral resolution images of the surface mineralogy,
(4) provide information on the morphology of the Martian surface, and
(5) characterize specific the Martian near-space radiation environment as related to radiation-induced risk to human explorers.

In addition, the project will provide for regular public release of imagery and other science/technology data via the Internet as well as regular releases for public information purposes.

1.4 Mars 2001 Operations Management

The Mars Exploration Program is managed for NASA by the Jet Propulsion Laboratory (JPL), California Institute of Technology. A JPL development project will oversee the design, building, and testing of the Mars 2001 orbiter by Lockheed Martin Astronautics (LMA) in their Denver, Colorado, facilities. JPL will also oversee launch of the spacecraft and operation of the spacecraft during the first month of flight, including deployment of solar arrays, establishment of telecommunications links and spacecraft flight control, and execution of trajectory course correction maneuvers to correct for launch bias and injection errors. Once in cruise, the orbiter will be operated by a spacecraft flight team at LMA and flight operations teams at JPL managed by the Telecommunications and Mission Operations Directorate (TMOD). This JPL/LMA team is also responsible for operation of the Mars Global Surveyor (MGS), even as the team assists development of future spacecraft elements of the MEP. TMOD also funds and manages operations by the science investigations and the initial analysis of data returned by the spacecraft and their scientific instruments. Science investigations on the Mars 2001 orbiter will largely be conducted remotely through the principal investigators' home institutions. These activities include both commanding of the science instruments and analysis of the returned instrument engineering and scientific data.

1.5 Mars 2001 Orbiter Measurement Synergies through Coordinated Operations Planning

The 2001 Mars Exploration Program Mission includes an orbiter with a gamma ray spectrometer, a multispectral thermal imager, and a radiation detector. An overview of these Mars 2001 science instruments is given in Table 1-1. The Mars 2001 Project Science Group (PSG) will provide coordinated planning and implementation of scientific observations. The PSG will also develop an archive plan that is compliant with Planetary Data System (PDS) standards and will oversee generation, validation, and delivery of integrated archives to the PDS.

Table 1-1. Mars 2001 Payloads

ORBITER		
THEMIS (Thermal Emission Imaging System	**THEMIS** will determine the mineralogy of the Martian surface using multispectral, thermal infrared images that have 9 spectral bands between 6.5 and 14.5 μm. It will also acquire visible-light images with 20 m/pixel resolution in either monochrome or color.	Philip Christensen, Arizona State University
GRS (Gamma Ray Spectrometer)	**GRS** will perform full-planet mapping of elemental abundance with an accuracy of 10% or better and a spatial resolution of about 300 km, by remote gamma ray spectroscopy, and full-planet mapping of the hydrogen (with depth of water inferred) and CO_2 abundances by remote neutron spectroscopy.	William Boynton, University of Arizona
MARIE (Martian Radiation	**MARIE** will measure the accumulated absorbed dose and dose rate tissue as a function of time, determine the radiation	Gautam Badhwar, Johnson Space

ORBITER		
Environment Experiment)	quality factor, determine the energy deposition spectrum from 0.1 keV/μm to 1500 keV/μm, and separate the contribution of protons, neutrons, and HZE particles to these quantities.	Center

1.6 Mars 2001 Project Science Group (PSG) Members

Raymond Arvidson (inter-disciplinary scientist)
Washington University
Department of Earth and Planetary Sciences
St. Louis, MO 63130

Email: arvidson@wunder.wustl.edu
Phone: (314) 935-5609
FAX: (314) 935-7361

Gautam Badhwar (MARIE PI)
NASA Johnson Space Center
Mail Stop SN3
2101 NASA Road 1
Houston, TX 77058-3696

Email: gautam.d.badhwar1@jsc.nasa.gov
Phone: (281) 483-5065
FAX: (281) 483-5276

William V. Boynton (GRS PI)
University of Arizona
Department of Planetary Science
Lunar and Planetary Laboratory
1619 E. University Blvd.
Tucson, AZ 85721-0092

Email: wboynton@lpl.arizona.edu
Phone: (520) 621-6941
FAX: (520) 621-6783

Philip Christensen (THEMIS PI)
Arizona State University
Department of Geology
Campus Box 871404
Tempe, AZ 85127-1404

Email: phil.christensen@asu.edu
Phone: (480) 965-7105
FAX: (480) 965-1787

Michael Meyer (program scientist)
NASA Headquarters
Code SR
Washington, DC 20546

Email: mmeyer@hq.nasa.gov
Phone: (202) 358-0307
FAX: (202) 358-3097

Jeffrey Plaut (deputy project scientist)
Jet Propulsion Laboratory
Mail Stop 183-501
4800 Oak Grove Drive
Pasadena, CA 91109

Email: plaut@jpl.nasa.gov
Phone: (818) 393-3799
FAX: (818) 354-0966

R. Stephen Saunders (project scientist)
Jet Propulsion Laboratory
Mail Stop 180-701
4800 Oak Grove Drive
Pasadena, CA 91109

Email: saunders@scn1.jpl.nasa.gov
Phone: (818) 354-2867
FAX: (818) 393-6546

2.0 MARS 2001 ORBITER OPERATIONS

2.1 Science Instruments

The Mars 2001 orbiter science payload consists of the Thermal Emission Imaging System (THEMIS), Gamma Ray Spectrometer (GRS), and Martian Radiation Environment Experiment (MARIE). The GRS instrument suite includes the gamma sensor head (GSH), neutron spectrometer (NS), and high-energy neutron detector (HEND). The locations of these instruments on the orbiter are shown in Figure 2-1. The GRS gamma sensor head is located on a 6-m boom, which is perpendicular to the orbit plane. The solar panel inner gimbal axis lies in the orbit plane and is collinear with the orbit velocity vector. THEMIS is oriented to observe in the nadir direction and GRS performs full-planet mapping. MARIE has a 68° field of view. Opportunities for science collection will be assigned on a time-phased basis depending on when conditions are most favorable to specific instruments.

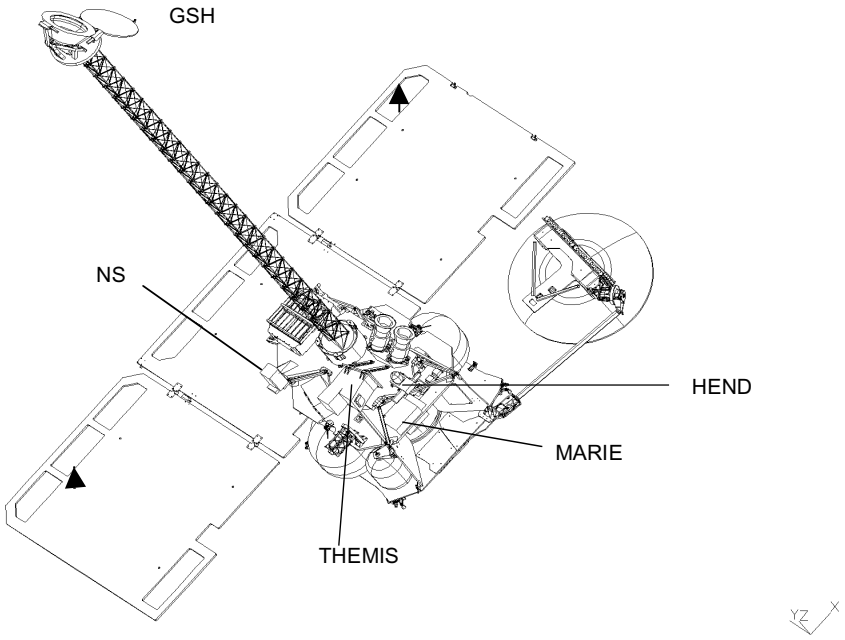

Figure 2-1. Orbiter Science Instruments

2.1.1 Thermal Emission Imaging System (THEMIS)

The Thermal Emission Imaging System (THEMIS) science objectives are to characterize the Martian surface environment by providing high-spatial and high-spectral-resolution mineralogical and morphological data by means of visible and infrared imagery. Mineralogical and morphological measurements will be obtained to determine a geologic record of past liquid environments. Mineral maps will be generated to obtain the mineralogy and petrology data to be used for identification of potential future Mars Surveyor Program landing sites. This experiment will provide essential information for the selection of future landing sites aimed at exobiologic exploration of Mars. The THEMIS Principal Investigator is Dr. Philip Christensen of Arizona State University.

The specific science objectives of the THEMIS experiment are to:

(1) determine the mineralogy and petrology of localized deposits associated with hydrothermal or subaqueous environments, and to identify sample return sites likely to represent these environments;

(2) provide a direct link to the global hyperspectral mineral mapping from the MGS thermal emission spectrometer (TES) by utilizing the same infrared spectral region at high (100 m) spatial resolution,

(3) study small-scale geologic processes and landing site characteristics using morphologic and thermophysical properties; and
(4) search for pre-dawn thermal anomalies associated with active subsurface hydrothermal systems.

THEMIS will determine surface mineralogy using multispectral thermal-infrared images in 9 spectral bands from 6.6 to 15.0 μm. The entire planet will be mapped at 100-m resolution within the available data volume because of our multispectral, rather than hyperspectral, imaging approach. THEMIS will also acquire 20-m resolution visible images in up to 5 spectral bands. Over 15,000 panchromatic (3,000 5-color), 20 × 20-km images will be acquired for morphology studies and landing site selection. The thermal-infrared spectral region contains the fundamental vibrational absorption bands that provide the most diagnostic information on mineral composition. All geologic materials, including carbonates, hydrothermal silica, sulfates, phosphates, hydroxides, silicates, and oxides have strong absorptions in the 6.6- to 15.0-μm region. Silica and carbonates, which are key diagnostic minerals in thermal spring deposits, are readily identified using thermal-IR spectra. In addition, the ability to identify all minerals allows the presence of aqueous minerals to be interpreted in the proper geologic context. THEMIS is designed as the follow-on to the Mars Global Surveyor TES, which will produce a hyperspectral (286-band) mineral map of the entire planet. THEMIS covers the same wavelength region as the TES, eliminating the need for additional hyperspectral mapping. Furthermore, the THEMIS filters will be optimized utilizing knowledge of Martian minerals determined from TES data, and TES global maps will allow efficient targeting of areas with known concentrations of key minerals. Remote sensing studies of natural surfaces, together with laboratory measurements, have demonstrated that 10 spectral bands are sufficient to detect minerals at abundances of 5 to 10%. More importantly, the absolute mineral abundance can be determined to within 15% using only 10 thermal-IR bands. The use of long-wavelength IR has additional advantages over shorter-wavelength visible and near-IR data because it can penetrate further through atmospheric dust and surface coatings, and the absorption bands are linearly proportional to mineral abundance, even at very fine grain sizes.

The quantitative mineral mapping objective will be met with a signal-to-noise ratio of 33 to 100. The instrument design will achieve this performance at the surface temperatures typical for the 4:30 p.m. orbit (235 to 265 K). In addition, the orbit is ideally suited to the search for pre-dawn temperature anomalies associated with active hydrothermal systems, whose discovery would radically alter our view of the current Mars. The instrument performance will detect temperature differences of only 1 K at 180 K. The visible imager will have a signal-to-noise ratio of >100 at 5:00 p.m. local time.

A critical aspect of the THEMIS design is the use of an uncooled microbolometer detector array for the IR focal plane. These detectors meet the science requirements while greatly simplifying the instrument design, spacecraft integration, ground testing, and flight operations. The optics consists of all-reflective, three-mirror anastigmatic telescope with an effective 12-cm entrance aperture and a speed of f/1.7. The IR and visible cameras share the optics and housing, but have independent power and data interfaces to the spacecraft. The IR focal plane has 320 cross-track pixels and 240 down-track pixels covered by ten 1-μm-wide strip filters. The array is clocked at 30 Hz, and 10 consecutive frames are co-added using time-delay integration providing a ground resolution of 100 m. The visible camera has a 1024 × 1024-pixel array with 5 filters. An internal flag provides calibration and Sun avoidance protection. The instrument weighs 10.7 kg, is 28 cm wide × 30 cm high × 31 cm long, and consumes an orbital average power of 5.1 W.

2.1.2 Gamma Ray Spectrometer (GRS)

The experimental objective of the GRS is to determine the elemental composition of the surface of Mars by full-planet mapping of elemental abundance with an accuracy of 10% or better and a spatial resolution of about 300 km by remote gamma ray spectrometry, and full planet mapping of the hydrogen (with depth of water inferred) and CO_2 abundances by remote neutron spectrometry. In addition, the instrument is also sensitive to gamma ray and particle fluxes from non-Martian sources and will be able to address problems of astrophysical interest including gamma ray bursts, the extragalactic background, and solar processes. The GRS Principal Investigator is Dr. William Boynton of the University of Arizona.

The GRS will detect and count gamma rays and neutrons emitted from the Martian surface. By associating the energy of gamma rays with known nuclear transitions and determining the number of gamma rays emitted from a given portion of the Martian surface, it is possible to calculate the ratio of elemental abundances of the surface and discern their spatial distribution. By counting the number of neutrons and segregating those in thermal and epithermal energy bins, it is possible to calculate the hydrogen abundance, thus inferring the presence of water. These data permit a variety of Martian geoscience and life science problems to be addressed, including the crust and mantle composition, weathering processes, volcanism, and the volatile reservoirs and processes.

The initial GRS activity will be to perform an instrument calibration before the boom is deployed. This activity will last between 15 and 40 days. The GSH, which uses a high-purity germanium detector cooled below 100 K to measure gamma ray flux, will be deployed on a 6-m boom (as shown in Figure 2-1) after 140 days in orbit, and will remain deployed for the duration of the mission.

GSH performance is a strong function of temperature, which constrains the spacecraft orbit beta angle (angle between orbit normal and direction to Sun) to insure that the GSH cooler is shaded from the Sun. The orbit beta angle must be less than –57.5° (–56° to shade cooler plus pointing uncertainty of 1.5°) in order to acquire quality data. Initial instrument calibration will be delayed until the beta angle geometry is satisfactory for GRS data acquisition. A periodic annealing of the germanium detector on the GRS may be required. Each annealing cycle takes approximately 7 days.

2.1.3 Martian Radiation Environment Experiment (MARIE)

The science objectives of MARIE are to characterize specific aspects of the Martian near-space radiation environment, characterize the surface radiation environment as related to radiation-induced risk to human exploration, and determine and model effects of the atmosphere on radiation doses observed on the surface.

The orbiter spectrometer will measure the energy from solar energetic particle (SEP) events as well as from galactic cosmic rays (GCR). This instrument will measure the elemental energy spectra of charged particles over an energy range of 15 to 450 MeV/n, over an angular acceptance cone of 50°. As the spacecraft orbits Mars, the axis of this cone sweeps through the sky. This instrument is provided by the Human Exploration and Development of Space (HEDS) Program in order to characterize the radiation environment at Mars.

2.2 Initial Science Orbit

The initial science orbit is attained after aerobraking is completed and maneuvers are performed to circularize the orbit. A near-circular orbit with a 400-km index altitude provides the observational geometry desired by the science instruments. The index altitude is the semi-major axis of the spacecraft orbit minus a representative mean radius of Mars (3397.2 km). The orbit period of just under 2 hours results in 12.5 spacecraft revolutions about Mars per sol. Successive ground tracks are separated in longitude at the equator by approximately 29.5°, and the entire ground track pattern nearly repeats every 2 sols. For each 2-sol repeat cycle, the ground track shifts a small amount (approximately 0.9°).

The initial orbit will be near-circular, but long-term gravitational perturbations will cause the orbit eccentricity to cycle from values near 0.0 to 0.023 with a period of about 74 days. The variation in planetographic altitude will range from 20 to 150 km. Unlike a frozen orbit, eccentricity and argument of periapsis will change with time.

Orbital elements at the completion of aerobraking are listed in Table 2-1. Note that a week will likely be required after the completion of aerobraking for systems checkout before nominal science phase activities can commence. The initial inclination is slightly greater than that required for a Sun-synchronous orbit, in order to allow the local mean solar time (LMST) of the orbit to slowly drift later as part of the orbit design strategy discussed in Section 2.3. The Mars season at the completion of aerobraking is summer in the southern hemisphere.

Table 2-1. Orbital Characteristics at Completion of Aerobraking (Launch at Open of Launch Period)

Epoch (GMT, ET)	Dec 8, 2001 05:00
Index Altitude (km)	400
Semi-major Axis (km)	3797.2
Period (min.)	118.4
Eccentricity	0.0
Inclination (deg)	93.1
Longitude of Ascending Node* (deg)	35.0
Argument of Periapsis* (deg)	0.0
Mean Anomaly (deg)	0.0
LTST of Descending Node (HH:MM)	4:13 p.m.
LMST of Descending Node (HH:MM)	4:43 p.m.
Solar Beta Angle (deg)	–52

* Mars Mean Equator/IAU of Date Nonrotating Coordinate Frame

2.3 Orbit Evolution

The science orbit design is optimized to balance the observational desires of THEMIS with those of GRS. The MARIE investigation does not directly affect the orbit design. At the start of the science orbit, the local true solar time (LTST) of approximately 4:13 p.m. allows high-quality THEMIS observations, but the beta angle of –52° prohibits acquiring GRS data. High-quality THEMIS infrared data are only obtained at local true solar times (LTST) earlier than 5:00 p.m. (Section 2.1.1) while high-quality GRS data are only obtained for beta angles less than –57.5°. THEMIS and GRS observations may continue outside of their optimal solar geometry, as power and telecom constraints allow.

The time-history of LTST and beta angle is controlled by changing the spacecraft orbit nodal precession rate (the rate at which the orbit plane rotates in inertial space). Figure 2-2 displays the time-history of the science orbit LTST and beta angle for the entire science and relay phases of the orbiter mission. The figure also includes LMST, scaled Mars-to-Earth range, and scaled declination of the Sun with respect to the Mars equator. LMST is a fictitious solar time that assumes that Mars moves in a circular orbit about the Sun with a period equal to the actual elliptical Mars orbit. LMST is constant for a Sun-synchronous orbit. Differences between LTST and LMST are due solely to Mars's non-zero heliocentric orbit eccentricity. The Mars-to-Earth range is the dominant factor in determining the Mars-to-Earth data rate, and the Sun declination indicates the Mars season. Note that the science orbit begins during southern summer on Mars.

The nodal precession rate is controlled by slight changes to orbit inclination. The inclination of the science orbit (see Table 2-1) is biased slightly higher than that required for Sun-synchronous precession to cause the beta angle to decrease (go more negative) so that GRS observations can commence early in the science mission. During the 917-day, primary science mission, the LMST drifts at a constant rate from its initial value of 4:43 p.m. to 5:05 p.m. The nominal science mission ends in June 2004. The end of the science mission coincides with the end of the second THEMIS opportunity.

Mars-to-Earth range is near the maximum during the first THEMIS opportunity but is near the minimum at the beginning of the second THEMIS opportunity. Therefore, more THEMIS data are transmitted to Earth during the second THEMIS opportunity. Quality GRS data acquisition commences approximately 120 days into the science orbit phase and continues until the end of the science mission. During this GRS observation period, the maximum beta angle is –54.7°. The GRS observation period spans more than a Mars year. MARIE can operate throughout the entire science mission of 917 days.

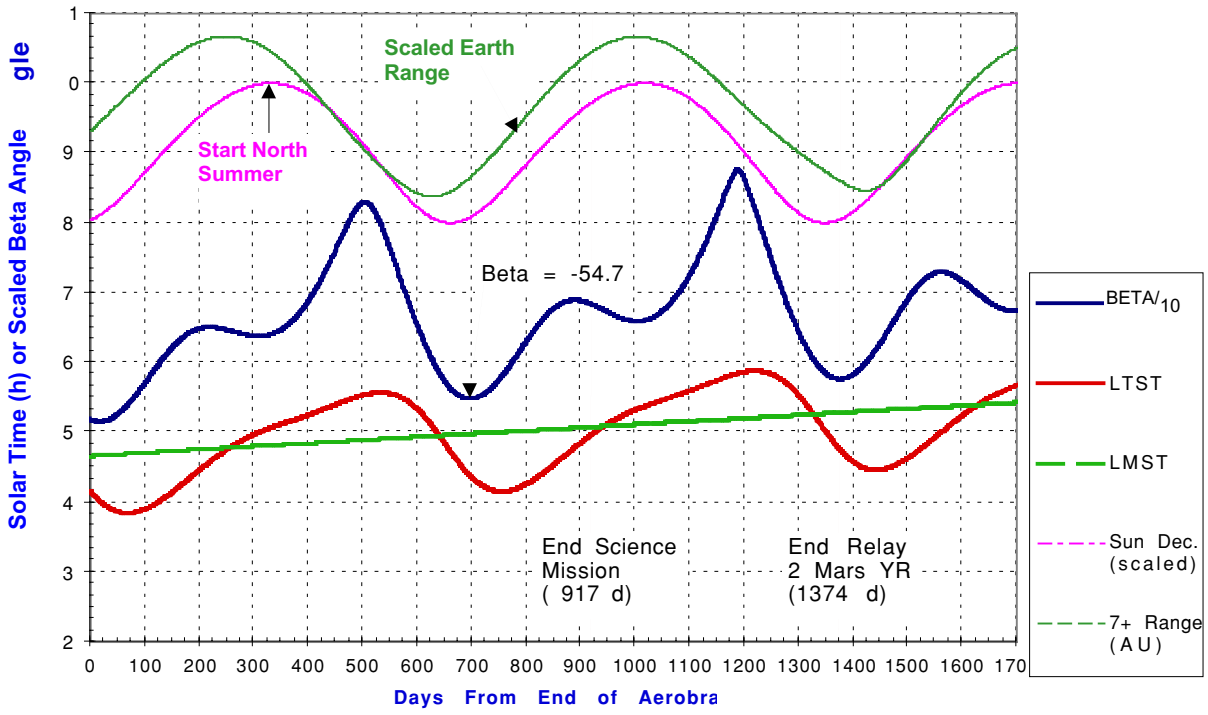

Figure 2-2. Science Orbit Evolution

The expected total science data volume to be returned during the orbiter science mission is shown in Table 2-2, compared with the data volumes contained in the Announcement of Opportunity Proposal Information Package (PIP) issued to the science community in April 1997. The science mission duration at the time of the PIP was 3 Earth years, compared with 917 days (2.5 Earth years) for the current mission. Despite this reduction in the science mission duration, the total expected orbiter data volume is more than double the PIP value. All orbiter science data will be archived in the Planetary Data System (PDS).

Table 2-2. Orbiter Science Data Volume

Instrument	Current Best Estimate of Data Volume (Gbits)	Proposal Information Package Data Volume (Gbits)
THEMIS	942	364
GRS	68	68
MARIE	3	3
Total	1,013	435

3.0 GAMMA RAY SPECTROMETER (GRS)

Note: The following is taken from a description of the Mars Observer Gamma Ray Spectrometer (Boynton et al. 1992). The 2001 instrument differs in implementation from the one described here, but the returned data and intended applications are nearly unchanged from the Mars Observer instrument.

The Mars 2001 GRS will return data related to the elemental composition of Mars. The instrument has both a gamma ray spectrometer and several neutron detectors. The GRS will return a spectrum nominally every 20 s from Mars, permitting a map of the elemental abundances to be made.

The gamma rays are emitted from nuclei involved in radioactive decay, from nuclei formed by capture of a thermal neutron, and from nuclei put in an excited state by a fast-neutron interaction. The gamma rays come from an average depth of the order of a few tens of centimeters. The spectrum will show sharp emission lines whose intensity determines the concentration of the element and whose energy identifies the element. The neutron detectors, using the fact that the orbital velocity of the spacecraft is similar to the velocity of thermal neutrons, determine both the thermal and epithermal neutron flux. These parameters are particularly sensitive to the concentration of hydrogen in the upper meter of the surface. By combining the results from both techniques it is possible to map the depth dependence of hydrogen in the upper meter as well. These data permit a variety of Martian geoscience problems to be addressed, including the crust and mantle composition, weathering processes, volcanism, and the volatile reservoirs and processes. In addition, the instrument is also sensitive to gamma ray and particle fluxes from non-Martian sources and will allow scientists to address problems of astrophysical interest, including gamma ray bursts, the extragalactic background, and solar processes.

3.1 GRS Instrumentation

The design of the GRS consists of two main components: the sensor head and the central electronics assembly. They are separated by a 6-m boom (Figure 3-1), which will be extended after the spacecraft enters the mapping orbit at Mars in order to minimize the spacecraft contribution to the gamma ray signal.

A cross section of the sensor head is shown in Figure 3-2. Its major components are the Ge detector assembly, the cooler subsystem, consisting of the cooler plate and V-groove thermal shield; and the anticoincidence shield/neutron detector (AC/N), consisting of the boron-doped plastic scintillator and photomultiplier tubes (PMTs). The sunshade, sunshade door, and preamplifier are not shown.

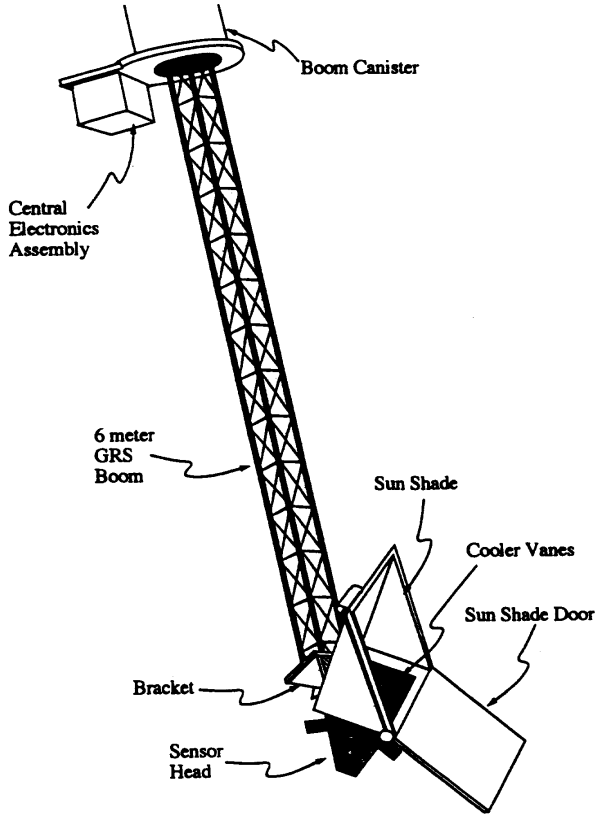

Figure 3-1. The Mars Gamma Ray Spectrometer (GRS). The sensor head is mounted on the end of a 6-m boom to separate it from the background gamma ray signal coming from the spacecraft and the GRS central electronics assembly.

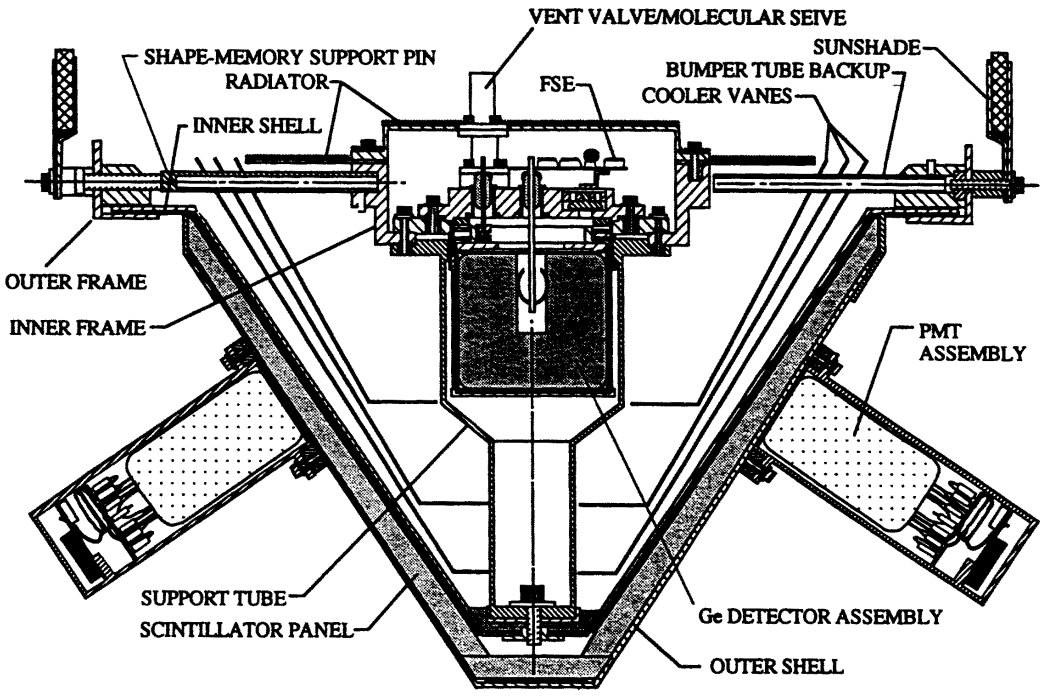

Figure 3-2. The Gamma Ray Spectrometer Sensor Head. The sensor head contains the Ge detector, the front stage electronics (FSE), and the surrounding scintillator panels and photomultiplier tubes (PMT) that compose the anticoincidence shield and neutron detector.

3.1.1 Gamma Ray Detector

The solid-state detector is a large single crystal of *n*-type ultrahigh-purity germanium (HPGe), about 5.5 cm in diameter and 5.5 cm long, with semiconductor electrodes implanted or diffused such that the crystal becomes a diode—that is, it will pass current in only one direction. The diode is operated in the reverse bias mode with a potential of about 3000 V and a leakage current of less than 1 nA. The detectors must be operated cold, less than about 130 K, to maintain high resolution and a low leakage current.

When a gamma ray photon interacts with the detector, hole-electron pairs are created that are quickly swept to the appropriate electrodes. This small charge is collected by a sensitive preamplifier and produces a pulse whose height (voltage) is proportional to the energy deposited in the crystal. This pulse is then shaped and amplified and passed to a pulse-height analyzer, which counts the events in the form of a histogram sorted according to the pulse amplitude, which is proportional to energy.

In the laboratory, HPGe detectors are generally operated near the boiling point of liquid nitrogen, 77 K; but in space it is difficult to attain this temperature, and the detector must be operated somewhat warmer. As mentioned above, detectors can normally operate at temperatures up to 130 K with little loss of energy resolution, but when they have been exposed to the radiation equivalent to about a one-year exposure in space, they need to be operated at 100 K or less (Brückner et al. 1990). If they are irradiated with a sufficiently high dose of energetic particles, such as neutrons or protons, HPGe detectors will have degraded resolution. During the mission the spacecraft and detector will be exposed to cosmic radiation for at least 3 years. As a result, the energy resolution of a detector will degrade to such a degree that it is substantially compromised for further measurements.

Brückner et al. (1991) incrementally exposed several large-volume *n*-type high-purity germanium detectors to a particle fluence of up to 10^8 protons cm^{-2} (proton energy = 1.5 GeV) to induce radiation damage. The detectors were held at operating temperatures of 89, 100, and 120 K to cover temperature ranges expected for the mission. They found that the resolution degradation was correlated with higher operating temperature. In addition, the peak shapes in the recorded gamma ray spectra showed a significant change from a Gaussian shape to a broad complex

structure. After a proton fluence equivalent to an exposure of 1 year in space, only the detector that was held at 89 K showed an energy resolution less than 3 keV; all other detectors had resolutions near or above 6 keV, a performance that is not adequate for high-resolution spectroscopy (Brückner et al. 1990).

The radiation damage can be removed by heating the germanium crystal to temperatures of the order of 370 K for several days. The GRS detector will operate at about 100 K, and thus we expect to anneal it with on-board heaters about once per year.

3.1.2 Anticoincidence Shield/Neutron Detector

The shield serves two purposes. The first is to "shield" the gamma ray sensor from the effect of charged particles. Because the gamma ray sensor detects any ionizing radiation, it is sensitive to charged particles as well as gamma rays. Rejecting the charged particle events electronically before they are recorded in the pulse height spectrum will improve the signal-to-noise ratio in the desired gamma ray signal. The instrument does this by looking for a simultaneous event in the shield and the gamma ray sensor. If the events are in coincidence, within 10 μs, the event in the gamma ray detector is assumed to be due to a charged particle, because the shield has a very low probability for a gamma ray interaction.

The second purpose of the shield is to determine the neutron flux at Mars. The plastic scintillator in the shield emits light when struck by ionizing radiation such as energetic charged particles. It is also doped with boron, an element with a high neutron absorption cross section, so that it can also generate a light pulse following neutron capture via the ^{10}B (n, α)^{7} Li reaction. PMTs detect this light and generate a pulse that is proportional to the amount of energy deposited in the plastic. The pulse from a neutron capture event has a characteristic electron-equivalent energy that generates a peak in the spectrum at about 80 keV. This peak can be distinguished from gamma ray events, which make a continuum, and cosmic ray events, which are typically 500 keV or more.

The shield consists of four planar trapezoids arranged in the shape of a pyramid. The orientation of the faces relative to the spacecraft velocity vector will be fixed throughout the mapping orbit. One face will view forward, one will view backward, and two will view sideward.

Separation of the thermal and epithermal components will be possible using the relative count rates of the shield faces and a Doppler-filter technique (Feldman and Drake 1986). Such a separation is made possible by the fact that the spacecraft will travel faster (3.4 kms^{-1}) than a thermal neutron (2.2 kms^{-1}) while in mapping orbit. The forward-directed shield face will therefore scoop up thermal neutrons, and the backward-directed face will outrun them. It was shown (Feldman et al. 1993) that count rate differences among the predominantly forward-, backward-, and sideward-directed faces (three faces are needed to yield two count rate differences) can be transformed to yield separate thermal and epithermal amplitudes of the planetary neutron leakage spectrum.

3.1.3 Radiative Cooler

The gamma ray sensor is cooled by emitting thermal radiation to space from the radiator plate. In order to better thermally isolate the sensor and radiator from the surroundings, a V-groove cooler design is being used for this mission (see Figure 3-2). In this design, the radiative heat leak to the cold stage is greatly reduced by an arrangement of lightweight, low-emittance, highly specular and reflective radiation shields (Bard et al. 1982; 1984). Large V-shaped cavities are created by arranging adjacent shields that expand outward from the cold stage (Bertsch et al. 1988). The shields intercept the radiation from the warm surroundings and, by multiple reflections, direct the energy to space. Parasitic conductive heat leaks are reduced by the use of low-conductance structural supports and memory-metal support pins that retract and disengage when cooled. Also included in the design are sunshades and a door to cover the radiator. This door, when opened, prevents radiation from the Martian surface from being seen by the cooling surfaces. When closed, the door allows the sensor to be heated for the annealing process. Because the spacecraft will be in a Sun-synchronous polar orbit, a fixed-position sunshield is used.

3.1.4 The Central Electronics Assembly (CEA)

The CEA contains all of the electronics associated with the GRS, except for the preamplifiers. It contains the power supplies, the main amplifiers, the analog-to-digital converters (ADCs), the gamma and neutron pulse height analyzers (PHAs), and the central processing units and memory. It is mounted on the canister that holds the 6-m boom and remains at this location; it does not travel with the sensor head as the boom is extended. The CEA remains with the spacecraft in order to reduce the mass at the end of the boom and to reduce the gamma ray contribution from this assembly that would otherwise contaminate the signal from Mars. The gamma PHA generates a spectrum by counting each photon that the detector sees. It contains an ADC that digitizes the height of each pulse, generating a number that is proportional to the energy deposited in the detector. This number is then used as an address of a memory location, or channel, corresponding to that energy. The PHA increments the value stored in that location and thus generates a spectrum that is a histogram of the number of events as a function of energy.

The gamma PHA uses a design that minimizes the number of channels of memory required to store a spectrum. Typically 4096 (4k) to 16384 (16k) channels are used for high-resolution Ge gamma ray spectra, with more channels used when a larger energy range is covered. The requirement on the number of channels is to provide a minimum of three channels per peak so that blended peaks can be deconvolved by software on the ground. Because the width of the peaks is determined, at least in part, by the statistical dispersion in the number of electrons collected for a given energy, it increases in proportion to the square root of the energy. Thus, fewer channels are required per unit of energy for the high-energy portion of the spectrum. A 14-bit number, with a range up to 16384 (16k), is generated by the gamma ADC; but if the number is 4k or more, it is divided by 2 and summed with 2k, to generate numbers in the range of 4k to 10k. Thus the lower 4k channels are stored with their normal width (nominally 0.6 keV/channel), but the upper 12k channels are compressed in width by a factor of 2. The resulting 10k spectrum saves 6k of on-board memory at the expense of a somewhat more difficult ground data processing scheme.

3.2 Mission Design and Data Analysis

3.2.1 Mission Design

At the start of the trans-Mars cruise, the spacecraft will deploy the GRS boom to the cruise position, about 2 m in the spacecraft nadir direction. This position will permit the cooler door to be opened, allowing the detector to cool. A greater extension is not permitted during cruise in order to maintain the correct spacecraft center of gravity for Mars orbit insertion (MOI). GRS will perform a 2-week checkout early in cruise, collecting astrophysical data such as cosmic gamma ray burst data during the cruise, as permitted by available Deep Space Network coverage and spacecraft power. The early checkout is required to get a baseline measurement of instrument performance before significant radiation damage has occurred and to examine the increase in intensity of radiation from short-lived radionuclides that are produced in the GRS, especially the Ge detector, from cosmic ray bombardment.

Prior to MOI, GRS will perform another two-week checkout to assess the effects of radiation damage on energy resolution and, if necessary, perform an anneal of the germanium crystal to recover the lost resolution. A postanneal checkout will be performed to assess the effectiveness of the anneal.

After MOI and prior to arrival into the mapping orbit, the spacecraft will move through the orbit insertion phase, a set of four highly elliptical drift orbits required to move the ascending node of a 2 p.m. local time orbit. The elliptical orbits of this insertion phase will provide GRS with its only opportunity to perform calibrations at varying Mars distances and at varying orbital velocities relative to the planet. The longest period of calibration will be a minimum of 21 days in the one-day drift orbit period. This calibration helps in characterizing the spacecraft signal from the total signal returned from the instrument.

Within several days of the start of the mapping phase the GRS boom will be reoriented from its cruise position, in the nadir direction, to its first intermediate mapping calibration position, in the direction of the spacecraft velocity vector. Calibration measurements of the background will then be performed at each of two boom extensions before the final mapping extension to the full 6-m length. These calibration measurements at different distances from the

spacecraft are needed to determine the background gamma ray flux from the spacecraft and will last about 2 to 4 weeks each. After the full extension of the boom, GRS will then be ready to begin collecting its science data.

3.2.2 Data Analysis

Figure 3-3 shows an example of a calculated spectrum of Mars based on a composition derived from the Viking results and the shergottite. It shows the characteristic sharp emission gamma ray lines superimposed on a continuum. The lines reflect gamma rays from discrete nuclear transitions that pass unattenuated to the detector through the intervening material, and the continuum is produced by Compton scattering of these gamma rays in both the intervening material or in the detector. Owing to the finite energy resolution of the detector, the lines are recorded as peaks that are generally Gaussian in shape (Yadav et al. 1989). The data are analyzed by first determining the energy and the area above the continuum for each peak. The energy identifies the element responsible for the gamma ray emission, and the area (number of counts) is proportional to the amount of that element in the surface. The determination of the proportionality constant that relates these counts in the spectrum to the concentration of the element is far from trivial, however.

The precise determination of the peak area in a gamma ray spectrum is essential for the determination of element concentrations. There are a number of peak-fitting routines, which perform a peak-area determination for laboratory gamma ray spectra. In prompt gamma ray spectrometry, the spectral shape of the gamma ray spectra is more complex, and certain peaks differ from the normal narrow Gaussian shape. Doppler broadening is usually the reason for these oddly shaped peaks. In addition, build-up of radiation damage in the HPGe detector gives rise to asymmetrical peak broadening.

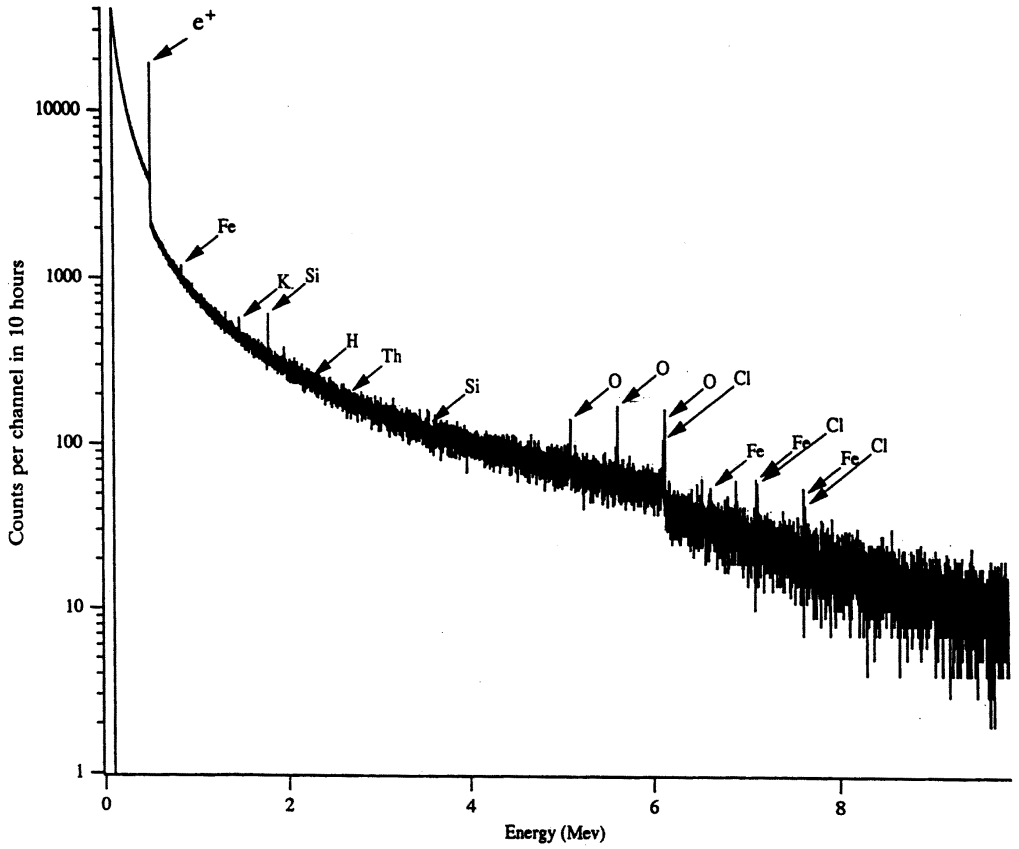

Figure 3-3. Calculated Gamma Ray Spectrum from Mars. The continuum is from gamma rays that are scattered in the surface, in the atmosphere, or in the instrument itself. The lines are from the gamma ray emissions from the elements indicated. The energy of the emission identifies the element, and the intensity of the line indicates the amount of the element present. The line labeled e+ is due to positron annihilation.

In addition to being able to deal with a number of different peak shapes, the peak-fitting algorithm must be able to accommodate weak peaks—those whose peak area is near the detection limit. The selected gamma ray evaluation code (GANYMED), which is a derivative of the code described by Kruse (1979), has the capability of fitting both weak and oddly shaped peaks. The method of computation of a standard peak is the following. First, the detector characteristic is designated; that is, its energy resolution as a function of energy, important for the evaluation of closely spaced peaks. Second, an automatic peak search is performed by applying a cross-correlation function. Then, the data points of the region of interest in the spectrum are fitted by an analytical function consisting of the sum of a polynomial background and a multiple-peak function. The latter is a Gaussian function with an exponential tailing on the low-energy side of the peak. A modified Gauss-Newton iterative algorithm is applied to the data set, and parameters are determined to calculate the peak area. The GANYMED code can evaluate a normal Gaussian peak with a small exponential tailing on the low-energy side, a Gaussian peak with an extended exponential tailing (as encountered for weakly radiation-damaged germanium detectors), and a Gaussian peak with an extended exponential tailing superimposed by a broad Gaussian bump (as encountered for heavily radiation damaged detectors) (Brückner et al. 1991). An option is available for oddly shaped peaks as specifically found in prompt gamma ray spectra (Brückner et al. 1987).

A study was done by Yadav et al. (1989) to investigate the weak-peak problem in high-resolution gamma ray spectroscopy. Knowing the shape of a peak a priori, for example, derived from a spectrum with good counting statistics, decreases the uncertainty of the peak area to some extent. To minimize the number of free parameters, the code provides the possibility to anchor the peak shape parameters, including the peak position; only the peak height is subject to the fitting algorithm. In this way the reliability of peak area determinations of weak peaks can be improved.

The number of counts in a peak depends on the efficiency of the detector. This parameter relates the probability that a photon of a certain energy striking the detector will register a count in the peak corresponding to that photon energy. Typical values range from about 20% at 1 MeV to 1.5% at 10 MeV. The losses are due to gamma rays passing through the detector with no interaction or scattering inside the detector with only a partial energy deposition. The flux of photons entering the sensor then must be corrected for the attenuation from the intervening material, which includes the detector packaging hardware as well as the planetary atmosphere, and for the solid angle of the planet relative to the instrument.

By far the most difficult task is the calculation of the relationship between the concentration of the element and the gamma ray flux at the surface from that element. This relationship depends on the succession of processes that are not measured directly but must be modeled or inferred from the measured gamma ray spectra. Because the neutron flux is dependent on composition, models are first used to estimate the concentration and computer calculations, then used to determine the neutron spatial and energy distributions from which a revised composition can be calculated. An iterative process is then used to determine both the final elemental composition and the neutron flux.

3.2.3 Spatial Resolution and Sensitivities

A key characteristic of the GRS data will be that individual spectra, typically acquired during 20-s integration intervals, will have inadequate signal-to-noise ratio to be statistically significant. Instead, they must be summed before geochemical information can be derived. As explained by Evans et al. (1993), the diameter of a spatial resolution element on the Martian surface is about 0.8 times the altitude, or 280 km. In fact, it takes many hours of accumulated data to yield a spectrum that can be analyzed to return composition results with reasonable uncertainty. Table 3-1 shows the time available to measure gamma rays above one spatial resolution element for the complete 687-day mission as a function of latitude. At high latitudes (80°) these accumulation times average 38 hours, while at the equator the accumulation times are less than 6 hours.

Table 3-2 gives the expected gamma ray count rates for 20 elements. These results were calculated using the neutron and gamma ray transport codes used by Evans and Squyres (1987). The results have been normalized to unity mass fraction, that is, 100% concentration of that element, so count rates for any other concentration can be readily obtained. The count rates cannot simply be scaled to obtain new results, however, because, as discussed above, changes in hydrogen content and in the composition of the surface affect the bulk neutron absorption cross

section. This in turn changes the neutron distribution and therefore the production of neutron capture gamma rays. Also in Table 3-2 are the expected background count rates and the resulting accumulation times required to measure the concentration of an element to 10% uncertainty. The values in Table 3-2 can be used to calculate sensitivities and uncertainties for other compositions and counting times. These parameters scale inversely with the square root of the counting time, and for lines that are small compared to the background, inversely with the concentration.

Table 3-1. Accumulation Times for the Gamma Ray Spectrometer for One Spatial Resolution Element*

Latitude	Hours
–80°	32.0
–60°	11.0
–40°	7.0
–20°	5.8
0°	5.7
20°	6.5
40°	8.7
60°	14.0
80°	44.0

*One spatial resolution element is 280 km × 280 km.

Table 3-2. Accumulation Time at Mars for 10% Relative Uncertainty in Concentration

Element	Energy, MeV	Mode*	Model Composition	Signal†	Background‡	Time, Hours
H	2.223	C	0.11%	1.5	0.024	300.0
C§	4.438	I	0.60%	0.0871	0.113	13000.0
N	10.829	C	2.8%	0.00190	0.00268	15000.0
O§	6.129	I	46.6%	0.0192	0.0079	6.1
Na	0.440	I	0.81%	0.249	0.105	730.0
Mg	1.369	I	3.7%	0.217	0.0403	21.0
Al	7.724	C	4.1%	0.0084	0.0040	1000.0
Si	1.779	I	21.5%	0.191	0.031	1.2
	3.539	C	21.5%	0.0198	0.0151	32.0
S	5.424	C	3.0%	0.0386	0.0091	210.0
Cl	6.111	C	0.70%	0.932	0.0080	15.0
K	1.461	N	0.12%	17.0	0.038	4.0
Ca	6.420	C	4.4%	0.0158	0.0067	440.0
Ti	1.381	C	0.38%	0.111	0.0059	990.0
Cr	8.884	C	0.15%	0.053	0.0028	13000.0
Mn	7.244	C	0.34%	0.105	0.0049	1100.0
Fe	7.632	C	13.5%	0.0455	0.0042	7.6
	0.847	I	13.5%	0.199	0.0689	3.9
Ni	8.999	C	52. ppm	0.106	0.00266	2.5×10^5
Gd	6.749	C	2.2 ppm	22.7	0.00616	69000.0
Th	2.614	N	0.45 ppm	9.05×10^3	0.020	40.0
U	0.609	N	0.13 ppm	1.77×10^4	0.092	500.0

* Mode refers to gamma rays produced by the processes of C (neutron capture), I (neutron inelastic scatter), and N (decay of natural radioactivity).
† Signal is in units of counts/second/mass fraction of the element.
‡ Background is in units of counts/second.
§ Only the contribution from the surface materials is considered.

Table 3-3 gives the calculated uncertainties for these 20 elements for both the 6-hour and 38-hour accumulation times. As can be seen, only elements with the highest gamma ray fluxes from Mars (oxygen, silicon, and iron) can be measured with less than 10% uncertainty in 6 hours. Many important minor and trace elements expected on Mars cannot be determined with less than 10% uncertainty even with 38 hours of accumulated data (e.g., hydrogen or aluminum). Results with uncertainties less than this can be obtained only with increased accumulation time

generated by adding surface resolution elements together. This increases the number of counts in a peak but at the expense of losing spatial resolution. This effect can be seen by comparing two synthetic spectra for Mars (Figure 3-4). The same small region of the spectrum is shown for two different accumulation times. In the 5.5-hour accumulation, only the potassium and silicon lines are visible, but in the 231-day accumulation, minor lines for other elements are also visible.

Table 3-3. Uncertainty in the Concentration at Mars for Two Accumulation Times

Element	Energy, MeV	Mode*	Model Composition	Uncertainty†, percent	
				6 Hours‡	38 Hours§
H	2.223	C	0.11%	70.0	28.0
C≠	4.438	I	0.6%	**	**
N	10.829	C	2.8%	**	**
O≠	6.129	I	46.6%	10.0	4.0
Na	0.440	I	0.81%	**	46.0
Mg	1.369	I	3.7%	19.0	7.7
Al	7.724	C	4.1%	**	54.0
Si	1.779	I	21.5%	4.5	1.8
	3.539	C	21.5%	23.0	9.2
S	5.424	C	3.0%	63.0	25.0
Cl	6.111	C	0.70%	16.0	6.4
K	1.461	N	0.12%	8.3	3.3
Ca	6.420	C	4.4%	92.0	37.0
Ti	1.381	C	0.38%	**	49.0
Cr	8.884	C	0.15%	**	**
Mn	7.244	C	0.34%	**	57.0
Fe	7.632	C	13.5%	11.0	4.6
	0.847	I	13.5%	8.1	3.2
Ni	8.999	C	52. ppm	**	**
Gd	6.749	C	2.2 ppm	**	**
Th	2.614	N	0.45 ppm	27.0	11.0
U	0.609	N	0.13 ppm	95.0	38.0

* Mode refers to gamma rays produced by the processes of C (neutron capture), I (neutron inelastic scatter), and N (decay of natural radioactivity).

† Uncertainties greater than 100% are indicated by double asterisks.

‡ Six hours corresponds to an accumulation time for one resolution element at the equator over the whole mission.

§ Thirty-eight hours corresponds to an accumulation time for one resolution element at 80° latitude over the whole mission.

≠ Contribution only from the surface material is considered.

One of the most important results for the GRS is the potential for detection and characterization of water on Mars. GRS determines water from the concentration of hydrogen. In order to measure hydrogen to 10% uncertainty, an accumulation time of 300 hours is required, as shown in Table 3-2. This time can be achieved by adding sufficient spatial resolution regions together. For a spacecraft in polar orbit, the accumulation time for a latitude band of a given width is independent of latitude. The required 300 hours corresponds to a latitude band 3° wide, accumulated over the entire mission. While results based on this type of accumulation would not provide a true map of hydrogen concentration, it would yield a determination of the hydrogen concentration as a function of latitude to the desired degree of uncertainty.

The above results apply only for the concentration of hydrogen assumed in the model: 0.11%, or equivalent to 1% water. If the hydrogen content over a particular geologic area is larger, then the results can be substantially improved. For example, for a hydrogen concentration of 0.33% (corresponding to a H_2O content of 3%), the uncertainties are 17% and 7% for accumulation times of 6 hours and 38 hours, respectively. In the polar regions of Mars the concentration of hydrogen might be quite high. For a concentration of 2.8% (corresponding to 25% water), the uncertainty for 38 hours is 1%.

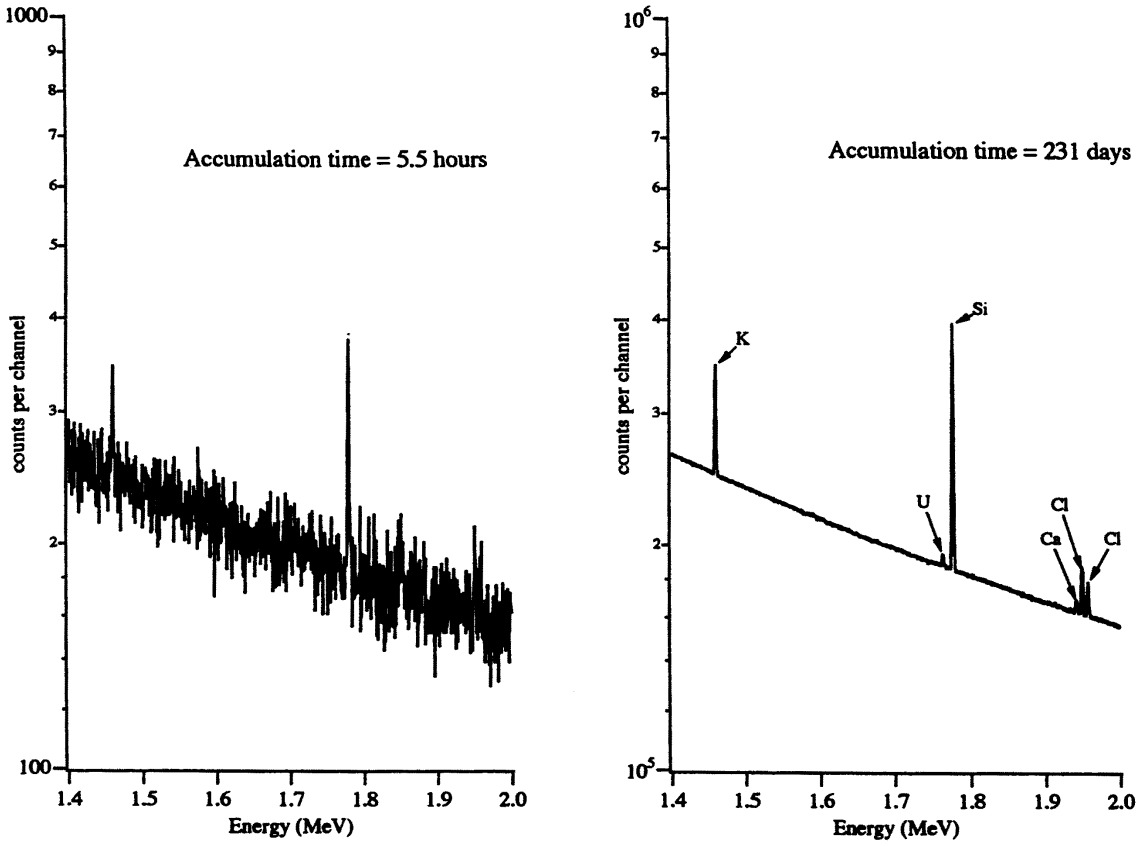

Figure 3-4. A Portion of the Simulated Spectrum for Mars with Two Different Accumulation Times. These spectra illustrate the effect of better sensitivities that can be obtained by combining pixels to get a longer accumulation time. The 5.5-hour accumulation (left) represents the expected time spent over a 280 km × 280 km pixel at the equator; the 231-day accumulation (right) represents the time that could be integrated to provide an average composition over a geologic region that is one third of the planet.

3.2.4 Reduction of GRS Neutron Data

The amplitudes of thermal and epithermal fluxes that leak upward from Mars are the primary information needed to infer the hydrogen content and its stratigraphy in near-surface layers, the thickness of carbon dioxide frost that covers the polar caps during winter, or the presence of sizeable deposits of carbonates near the surface of Mars. Although possible for some types of neutron detectors, these amplitudes cannot be determined directly from the measured count rates of individual AC/N shield faces of GRS. They can, however, be derived by combining the data from different faces as outlined next. A more complete description is given by Feldman et al. (1993).

Expected background and foreground count rates. The first stage of reduction involves a determination of counts that result from neutron capture by the boron contained in the scintillator faces of the AC/N subsystem. The spectrum of light output from the AC/N trapezoid resulting from background interactions is expected to be a broad continuum, dominated at low amplitudes by gamma rays and at high amplitudes by penetrating charged particles. In contrast, the spectrum resulting from low-energy neutron absorption will be peaked because of the high energy of the emitted α particle in the $^{10}B(n, \alpha)^7$ Li reaction relative to the energy of the absorbed neutron. An example of such a spectrum measured at Los Alamos National Laboratory using one of the protoflight trapezoids of GRS is shown in Figure 3-5. The peaked nature of this spectrum allows separation of neutron counts from background counts in spectra measured in Mars orbit through use of the measured calibration spectrum in Figure 3-5 and a least squares fitting routine. Whereas the background counts under the portion of the neutron peak that will be used in the fit is estimated to be about 35 s^{-1}, due to planetary neutrons it is estimated to range between 5 s^{-1} and 50 s^{-1}. The large range of estimated neutron count rates reflect different surface chemistries as well as differences in the

orientation of the trapezoid faces; for example, the backward-looking face outruns thermal neutrons and so will register the fewest planetary neutron counts.

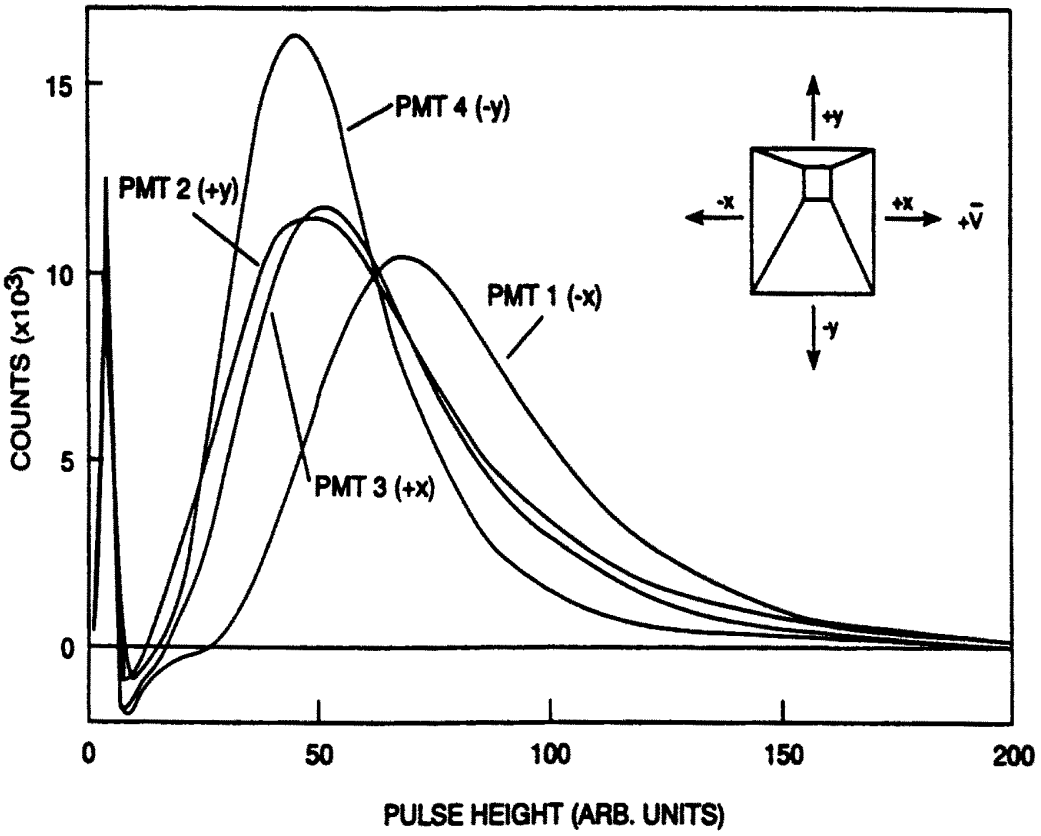

Figure 3-5. Energy Flux Spectrum of the $^{10}B(n, \alpha)^{7}$ Li Neutron Capture Reaction in Each Trapezoid of the Anticoincidence Shield/Neutron Detector. The peak at about 80 eV due to the neutron interactions can be resolved from the low-probability gamma reactions, which generate a continuum, and the charged particle interactions, which are at much higher energy. PMT is the photomultiplier tube.

Adjustment for surface area response functions. Because the separate faces of the AC/N subsystem have different orientations relative to the velocity vector of the spacecraft, they respond preferentially to neutrons evolving from different surface areas of Mars. This effect is shown in Figure 3-6. Inspection shows that each response function is offset from the nadir point and from each other. The response contours of the forward-looking face, J_{+}, is offset in the forward direction, that of the backward-looking face, J_{-}, is offset in the backward direction, and those of the two sideward-looking faces, J_{01} and J_{02}, are offset toward their respective view directions. Thus, the next step in the neutron data reduction chain must be to rearrange the neutron counts measured by each of the trapezoid faces during successive 20-s intervals to form quartets of individual-face response functions that maximally overlap the same surface region.

Further study of Figure 3-6 shows that the size of the surface response function, about 8° full width at half maximum, is comparable to the sizes of the Martian polar caps. This angular distance corresponds to about 480 km on the surface of Mars. Because photomosaic maps of Mars from Viking show many other regional features that have sizes of this scale or smaller, we expect that neutron count rates may vary significantly as a function of orbital location. Variations in measured count rates will therefore not reflect actual variations in leakage neutron fluxes but will appear more muted. Inversion of the raw rates to obtain thermal and epithermal amplitudes using an algorithm based on simulations of a globally uniform chemistry will therefore incorrectly identify these amplitudes. A specific example of this effect, tailored to the measured configuration of the south polar cap of Mars, was presented by

Feldman et al. (1993). Minimization of errors therefore requires a deconvolution of measured in-track, as well as cross-track, count rate variations before an accurate count rate inversion can be performed.

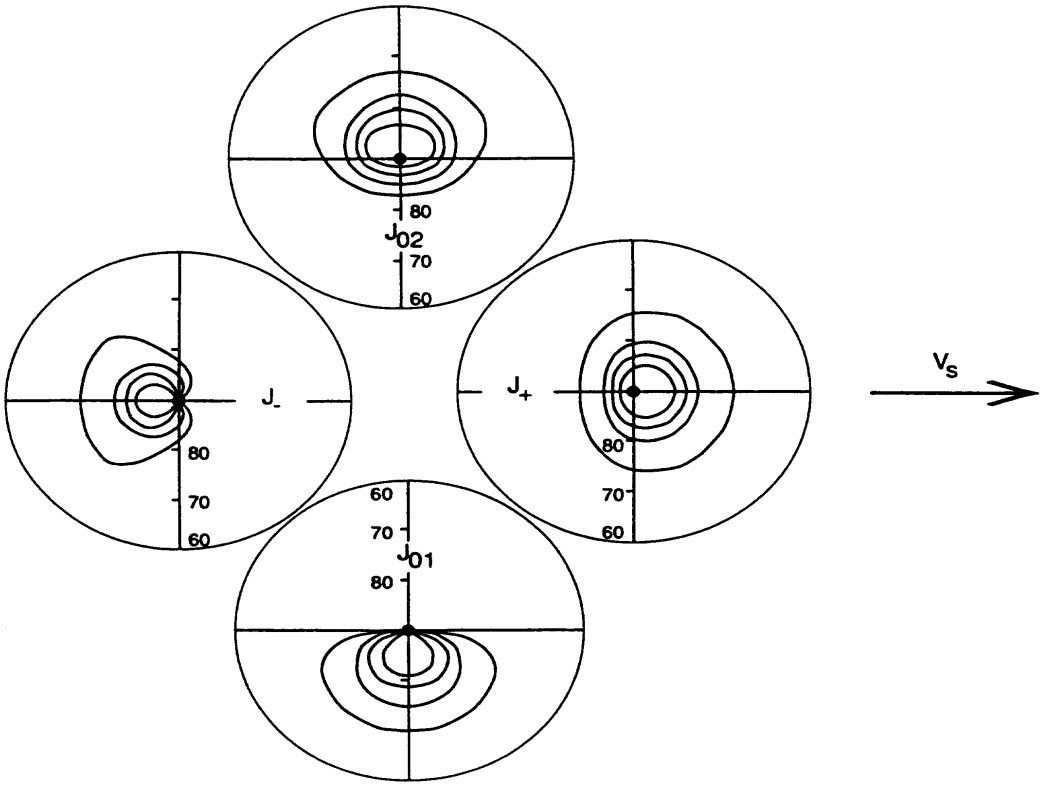

Figure 3-6. Contours of the Neutron Response Functions of the Four Individual Faces of the Gamma Ray Spectrometer Anticoincidence Shield/Neutron Detector Subsystem Relative to the Subsatellite Point. The subsatellite ground point is given by a large dot in the center of each diagram. The contour levels correspond to fractional maximum response values of 0.467, 0.330, 0.200, and 0.067, and the radial tick marks on the vertical axes correspond to the polar angle displacement from the nadir referenced to a planetary coordinate system having polar axis through the subsatellite point.

Inversion of count rates to determine thermal and epithermal amplitudes. Several studies of simulated neutron leakage fluxes from Mars have shown that resultant energy spectra can be fit well by a function of the form (e.g., Drake et al. 1988; Dagge et al. 1991).

$$F_m = \alpha(K/T) \exp(-K/T) + \beta(K/K_o)^{-p} F_c(K/K_o). \quad (1)$$

Here F_m is the model flux or current function, K is the neutron kinetic energy, α is the thermal amplitude, T is the temperature of the thermal distribution, β is the epithermal amplitude, p is the epithermal power law index, $F_c(K/K_o)$ is an arbitrary cutoff function to facilitate separation of thermal and epithermal components of F_m, and K_o is an arbitrary constant. Experimentation with many simulations showed that a cutoff function of the form

$$F_c(K/K_o) = [1 + (K/K_o)^{-k}]^{-1} \quad (2)$$

provided both good fits to simulated spectra and clean thermal-epithermal separations with the choices of K_o = 0.15 eV and k = 5.

Count rates of the faces of the AC/N subsystem of GRS were calculated for an extensive set of assumed Martian surface chemistries using a calculated energy-dependent efficiency function (Feldman et al. 1993). Best-fit thermal and epithermal amplitudes, α and β from (1), were also calculated for each of the simulated neutron spectra. Inter-

comparison showed that both individual calculated sensor count rates and differences in calculated sensor count rates could be well represented by an equation of the form

$$J_R(1) = a_T(1)\ \alpha_T + b_T\ (1)\ \beta_T. \tag{3}$$

Here $J_R\ (1) = (J_{+R} - J_{-R})$; $J_R(2) = (J_{0R} - J_{-R})$; $J_R(3) = J_{-R}$; $J_{0R} = (J_{01R} + J_{02R})/2$, and α_T and β_T are the thermal and epithermal amplitudes determined from fits of (1) to the calculated upward neutron leakage current at the top of the atmosphere. All J_R are, of course, evaluated at the orbital altitude of the spacecraft. A summary of the correlation given by (3) is shown in Figure 3-7. The fits to straight lines appear to be quite good. Because the slopes of the two upper difference count rates are sufficiently different, inversion of the measured $J_R(1)$ to determine α_T and β_T is possible. Use of the two count rate differences shown in Figure 3-7 is preferable to using a single face, since they will eliminate important systematic uncertainties introduced by imprecise knowledge of the background spectrum, which is produced by the interaction with the AC/N trapezoids of penetrating charged particles and of gamma rays and fast neutrons from Mars. Although this background will depend on both time and location, at any instant they should be nearly the same for each of the AC/N trapezoid faces. In the case where backgrounds can be determined accurately during the transition orbit phase of the mission, however, Figure 3-7 shows that the combination of $(J_+ - J_-)$ and J_- provide the best inversion accuracy. In fact, the nearly horizontal fit of J_-/β_T to a straight line shows that J_- is nearly independent of α_T and so provides an accurate measure of β_T by itself. This result reflects the fact that the orbital velocity of the spacecraft is sufficiently large that thermal neutrons cannot catch up to the spacecraft to register a count in the backward-facing trapezoid. Once β_T is known from J_-, then it is straightforward to use $(J_+ - J_-)$ to determine α_T.

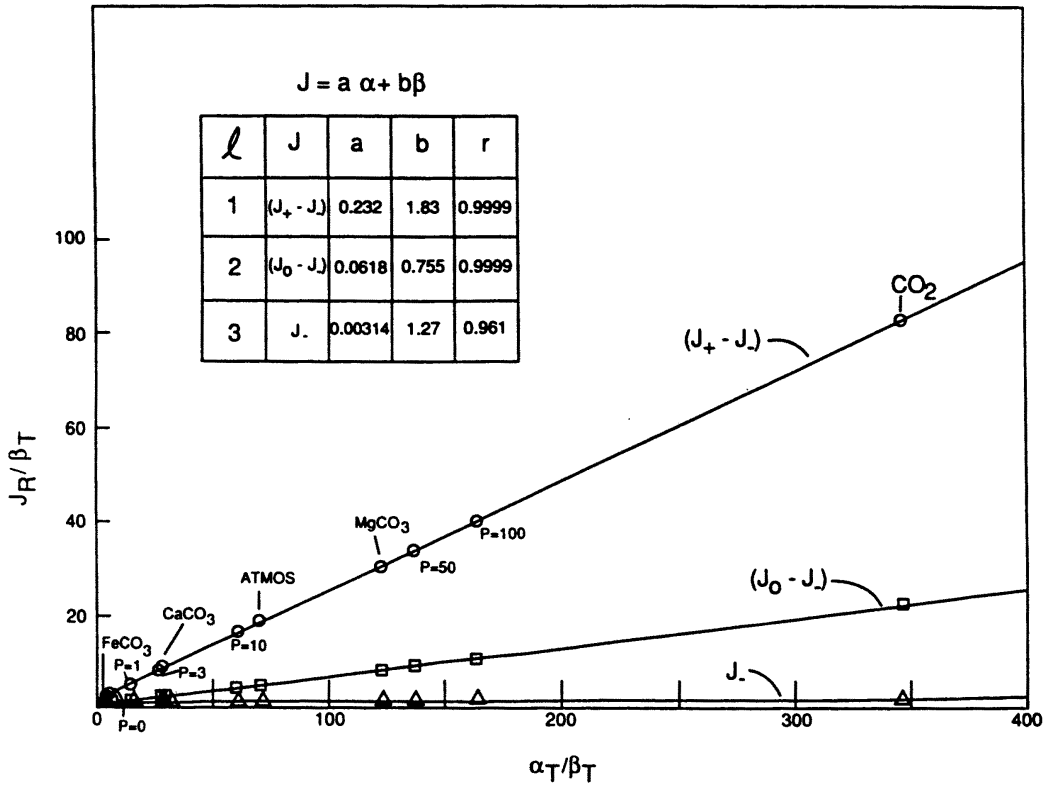

Figure 3-7. A Summary of the Correlation Given by Equation (3). The points labeled by *P* indicate a composition that is Martian soil with the indicated percentage of water. Inspection shows that the slopes of the two upper difference count rates are sufficiently different to allow inversion of the measured *J* to determine α_T and β_T.

4.0 THERMAL EMISSION IMAGING SYSTEM (THEMIS)

The THEMIS instrument will be used to provide thermal infrared and visible images of the surface of Mars throughout the science phase of the Mars 2001 mission.

THEMIS science measurements:

- emitted radiance: 6.6 to 15.0 μm in nine 1-μm bands at 100-m spatial resolution;
- detectors: multi-spectral imager = 320 × 320 uncooled, visible = 1024 × 1024 silicon array;
- f/1.7 telescope, infrared FOV = 4.6° crosstrack × 3.5° downtrack, and 2.9°-square visible array;
- resolution = 100 m (infrared) and 18 m (visual); and
- NEΔT @ 180 K = 1 K (IR), SNR >100 (visual).

4.1 Scientific Objectives

To contribute to the success of the scientific objectives of the Mars 2001 mission, the THEMIS will:

- determine the mineralogy and petrology of localized deposits associated with hydrothermal or subaqueous environments, and identify sample return sites likely to represent these environments;
- provide a direct link to the global hyperspectral mineral mapping from the Mars Global Surveyor TES by utilizing the same infrared spectral region at high (100-m) spatial resolution;
- study small-scale geologic processes and landing site characteristics using morphologic (18-m spatial resolution) and thermophysical properties;
- search for pre-dawn thermal anomalies associated with active subsurface hydrothermal systems.

4.2 THEMIS Baseline Design

THEMIS will determine surface mineralogy and thermophysical properties using multispectral thermal-infrared images in nine spectral bands from 6.6 to 15.0 μm. The entire planet will be mapped at 100-m spatial resolution within the available data volume by using a multispectral imaging approach. THEMIS will also measure 18-m spatial resolution surface morphology using multispectral visible imaging in five spectral bands from 423 to 870 nm. Over 15,000 panchromatic (3,000 five-color) 20 × 20 km images will be acquired for morphology studies and landing site selection. The combined infrared/visible imager is a spacecraft body-mounted push-broom, multi-spectral sensor with co-aligned infrared and visible fields of view (FOV). The THEMIS instrument will be comprised of two sensor assemblies, the infrared subsystem (IRS) and the visible imaging subsystem (VIS), each using its own dedicated electronic subsystem and sharing common optical and mechanical subsystems.

The THEMIS IRS and VIS will each use its own independent focal planes, read-out, data processing, data interface, and power supply electronics. The IRS electronics will provide digital data collection and processing as well as the instrument control and data interface to the spacecraft of the infrared data stream. Both the IRS and VIS will utilize commercial off-the-shelf electronics with only minor modifications (primarily to packaging) to accommodate space environmental requirements.

4.2.1 Infrared Subsystem (IRS)

The IRS design will include the infrared imaging subsystem (IRIS) and IRS electronics.

The IRIS will include the infrared detective assembly (IRDA), which is comprised of the infrared focal plane, thermal electric cooler, and spectral stripe filters, and the IR camera electronics. The IRDA will include an un-cooled micro-bolometer detector array for the infrared focal plane. The micro-bolometer array will contain 320 pixels cross-track by 240 pixels along-track, with a 50-μm pitch. The array's temperature will be controlled by the small IRDA thermal electric cooler that stabilizes the detector temperature to nominally ±0.002 K. Spectral discrimination in the infrared will be achieved with the IRDA spectral filters that are mounted directly over the focal plane. The IRDA will use nine 1-μm wide narrowband stripe filters in the 6.6 to 15.0 μm range. Each stripe filter

will cover the entire cross-track width of the array and 48 pixels (32 pixels clear aperture) in the along-track direction for the shortest wavelength filter and 24 pixels (16 pixels clear aperture) in the along-track direction for the remaining spectral filters. The array will be clocked out at effective frequency of 30 Hz. In order to increase the SNR, 16 consecutive frames will be co-added using time-delay integration. The resulting ground spatial resolution will be 100 m for each of the spectral bands. The IR camera electronics will provide ultra-stable, low-noise clock and bias signals to the focal plane, control of the thermal electric cooler, and will perform the initial analog and digital processing of the data stream.

The IRS electronics will include the command and control, timing and sequencing, shutter control, post-processing, spacecraft interface, and power conditioning electronics. The command and control electronics will process the commands from the spacecraft that control the operation of the IRIS and IRS electronics. The timing and sequencing electronics will generate the control timing clocks for the operation of the IRIS with the IRS electronics. The shutter control electronics will control the operation of the IRS shutter assembly. The post-processing electronics will supply final processing of the IRIS data, including the (16:1) time delay integration (TDI) processing, and lossless (~2:1) data compression using a Rice data compression algorithm. The spacecraft interface electronics will provide the final data formatting and data interface to the spacecraft. The power conditioning electronics will use DC-to-DC converters to perform the necessary power conditioning for the IRIS and IRS electronics. The power conditioning electronics will use off-the-shelf converters and discrete input filtering components to assure electromagnetic compatibility with the rest of the spacecraft.

The THEMIS sequencing software running on the spacecraft processor will perform the sequencing of the IRS image acquisition, including band selection and image length. The THEMIS data processing software running on the spacecraft processor will perform final Consultative Committee for Space Data Systems (CCSDS) data stream packetization of the IRS data.

4.2.2 Visible Imaging Subsystem (VIS)

The VIS design will include the VIS sensor and VIS electronics.

The VIS sensor design will use a 1024×1024–2.6×6.2 µm pixel (1018×1008 photoactive), 9-µm pitch CCD for the visible focal plane. Spectral discrimination in the visible will be achieved by mounting five filters directly to the detector. The five 50-nm wide narrowband stripe filters are distributed over the 423 to 870 nm range. Each stripe filter will cover the entire cross-track width of the array and ~200 pixels in the along-track direction. Band selection will be accomplished by selectively reading out only part of the resulting frame for transmission to the spacecraft computer. The entire detector array will be read out every 1.3 s, which will provide a ground spatial resolution of 18 m.

The VIS readout electronics will generate the clocks, biases, CCD sampling clock, and A/D conversion clock signals. These electronics will also perform direct current (DC) offset correction, amplification, and the A/D conversion. The VIS digital electronics will perform correlated double sampling subtraction, lossless (2:1) data compression using a first-difference Huffman data compression algorithm, initial data formatting, and storage of the visible data stream into internal memory until the spacecraft is ready to receive the data. The VIS spacecraft interface electronics will provide the data interface to the spacecraft and the command interface from the spacecraft to the VIS. The power conditioning electronics will use DC-to-DC converters to perform the necessary power conditioning for the VIS electronics. The power conditioning electronics will use off-the-shelf converters and discrete input filtering components to assure electromagnetic compatibility with the rest of the spacecraft.

The THEMIS sequencing software running on the spacecraft processor will perform the sequencing of the VIS image acquisition including band selection and image length. The THEMIS data processing software running on the spacecraft processor will perform final data stream compression and packetization of the VIS data stream for the CCSDS.

4.2.3 Optical Subsystem

The THEMIS will use a fast, wide field of view (FOV), reflective telescope in order to accommodate the infrared and visible bands performance with a single telescope. The 80 mrad × 60 mrad FOV will be achieved with an all-reflective, three-mirror f/1.7 anastigmatic telescope with an effective aperture of 12 cm and an effective focal length of 20 cm. The design will incorporate baffling to minimize stray and scattered light. The visible signal will be re-directed to the visible focal plane using a dichroic beamsplitter. The thermal infrared signal will be passed through this beamsplitter on its way to the infrared focal plane. The system will be optimized to match the high signal performance required for the IRS and the high spatial resolution required for the VIS. The 50-µm pitch of the IR focal plane array will map to a ground sampling distance (GSD) of 100 m. The system will produce a noise equivalent delta emissivity (NE$\Delta\varepsilon$) of about 0.025 in the infrared. Similarly, the 9-µm pitch of the visible array will map to a GSD of 18 m with a modulation transfer function (MTF) of approximately 0.2 at Nyquist. A full-field shutter will provide DC-restore capability of the IRS, and will also be used to protect the detectors from unintentional direct illumination from the Sun when the instrument is not in use.

4.2.4 In-Band Spectral Response

The IRS will collect infrared images in nine thermal infrared bands. The spectral characteristics of each band pass filter are listed in Table 4-1.

Table 4-1. THEMIS Infrared Band Characteristics

Band	Center Wavelength	Bandwidth (Full Width Half Power)
1/2	6.62 µm	1.01 µm
3	7.88 µm	1.09 µm
4	8.56 µm	1.18 µm
5	9.30 µm	1.18 µm
6	10.11 µm	1.10 µm
7	11.03 µm	1.19 µm
8	11.78 µm	1.07 µm
9	12.58 µm	0.81 µm
10	14.96 µm	0.86 µm

4.2.5 Out-of-Band Spectral Response

For each spectral band, the IRS response to wavelengths outside the band (out-of-band) will be less than 1% of the response to wavelengths inside the band (in-band). Out-of-band radiation is defined as the radiation from 1.8 to 50 µm that is outside 1.5 times the FWHM wavelengths for the band. In-band radiation is defined as the radiation that is within 1.5 times the FWHM wavelengths for the band. The spectral distribution of the source radiation is defined by a 245-K blackbody combined with a 5900-K greybody with an emissivity of 1×10^{-5}.

4.2.6 Spectral Sensitivity

The IRS spectral sensitivity will be such that for a 245-K blackbody thermal radiance from the surface of Mars ($\varepsilon = 1$), THEMIS will achieve the SNR's in Table 4-2.

Table 4-2. THEMIS Infrared Band Signal-to-Noise Ratio

Band	Center Wavelength	Measured SNR
1/2	6.62 µm	50
3	7.88 µm	110
4	8.56 µm	169
5	9.30 µm	190
6	10.11 µm	180
7	11.03 µm	200
8	11.78 µm	170
9	12.58 µm	130
10	14.96 µm	120

4.2.7 Instantaneous Field of View (IFOV)

The IRS instantaneous field of view will be 227 ±10 µrad in the cross-track direction and 123 ±10 µrad in the along-track direction.

4.2.8 Ground Sampling Distance (GSD)

The IRS ground sampling distance will be 100 ±10 m at a spacecraft altitude of 400 km.

4.2.9 Field of View (FOV)

The IRS will have 320 pixels in the cross-track direction in order to collect acceptable images and 240 pixels in the along-track direction to allow for nine spectral bands with (16:1) TDI. The resulting IRS field of view will be 80 ±5 mrad (4.58°) in the cross-track direction and 60 ±5 mrad (3.44°) in the along-track direction.

4.2.10 Total Encircled Energy

With the IRS instantaneous field of view, normalized total encircled energy will be as shown in Table 4-3.

Table 4-3. IRS Total Encircled Energy

Sensing Area (µrad square)	Minimum Normalized Response
250	0.85
750	0.95
1250	0.99

4.2.11 Modulation Transfer Function (MTF)

The IRS system modulation transfer function will be at least 0.2 at the Nyquist frequency for all field angles.

4.2.12 Dynamic Range

The IRS dynamic range will be adjustable in order to achieve a response that is digitized to 8 bits, full scale when viewing a 310-K blackbody spectral distribution integrated from 1.8 to 18 µm.

4.2.13 Linearity

The IRS linearity will be known within 5% of the full-scale signal in all bands.

4.2.14 Transient Response

The IRS transient response will settle to within 85% of its final value when the output changes over the full dynamic range within one frame.

4.3 VIS Performance

The VIS will provide the following performance characteristics in the visible spectral range.

4.3.1 In-Band Spectral Response

The VIS will collect visible images in five visible bands. The spectral characteristics of each band pass filter are listed in Table 4-4. The bandwidth is defined as the full-width at half-maximum points (FWHM).

Table 4-4. THEMIS Visible Band Characteristics

Band	Center Wavelength	Bandwidth (Full Width Half Power)
1	0.870 µm	0.05 µm
2	0.423 µm	0.05 µm
3	0.652 µm	0.05 µm
4	0.751 µm	0.05 µm
5	0.553 µm	0.05 µm

4.3.2 Out-of-Band Spectral Response

For each spectral band, the VIS response to wavelengths outside the band (out-of-band) will be less than 5% of the response to wavelengths inside the band (in-band). Out-of-band radiation is defined as the radiation from 0.3 to 1.1 µm that is outside 1.5 times the FWHM wavelengths for the band. In-band radiation is defined as the radiation that is within 1.5 times the FWHM wavelengths for the band. The source radiation is defined by a fixed-intensity, uniformly distributed target of known radiance and spectral distribution over 0.3 to 1.1 µm.

4.3.3 Spectral Sensitivity

The VIS spectral sensitivity will be measured at the system level. As a goal, the VIS spectral sensitivity will be such that for a low albedo (0.1), solar incidence angle of 75°, aphelion illumination conditions, flat surface at a 5 p.m. orbit, and the optical throughputs listed in Table 4-5, THEMIS will achieve the following SNRs at full spatial resolution.

Table 4-5. VIS Spectral Sensitivity

Band	Center Wavelength (nm)	Telescope Throughput	Beamsplitter Throughput	SNR
1	870	0.75	0.80	10
2	423	0.89	0.80	15
3	652	0.89	0.80	25
4	751	0.80	0.80	10
5	553	0.92	0.80	40

4.3.4 Instantaneous Field of View (IFOV)

The VIS instantaneous field of view will be 13 ±1.3 µrad in the cross-track direction and 31 ±3 µrad in the along-track direction.

4.3.5 Ground Sampling Distance (GSD)

The VIS ground sampling distance will be 18 ±2 m at a spacecraft altitude of 400 km.

4.3.6 Field of View (FOV)

The VIS will have at least 1000 pixels in the cross-track direction in order to collect acceptable images and at least 1000 pixels in the along-track direction to allow for five spectral bands with about 200 pixels per filter. The resulting VIS field of view will be at least 80 mrad (4.58°) in the cross-track direction and at least 60 mrad (3.44°) in the along-track direction.

4.3.7 Total Encircled Energy

With the VIS instantaneous field of view, normalized total encircled energy will be as shown in Table 4-6.

Table 4-6. VIS Total Encircled Energy

Sensing Area (μrad square)	Minimum Normalized Response
45	0.85
135	0.95
225	0.99

4.3.8 Modulation Transfer Function (MTF)

The VIS system modulation transfer function will be at least 0.1 at the Nyquist frequency for all field angles.

4.3.9 Dynamic Range

The VIS dynamic range will be measured at the system level. The VIS dynamic range will be adjustable in order to achieve a response that is digitized to 8 bits, full scale when viewing a target with an albedo of 1.0.

4.3.10 Linearity

The VIS linearity will be measured at the system level. The VIS linearity will be determined to within 5% of the full-scale signal in all bands.

4.4 IRS and VIS Sensor Co-Registration

The IRS and VIS will be co-aligned so that their optical axes are within ±1 mrad to allow co-registration of the infrared and visible images.

4.5 Pointing and Alignment

The pointing accuracy of the IRS and VIS will be within ±5 mrad of the alignment cube to allow for targeting. The pointing knowledge of the IRS and VIS will be within ±1 mrad of the alignment cube to allow for image reconstruction.

5.0 MARTIAN RADIATION ENVIRONMENT EXPERIMENT (MARIE)

Space radiation presents a very serious hazard to crews of interplanetary human missions. The two sources of this radiation are the galactic cosmic rays (GCR) and solar energetic particle (SEP) events. The GCR provides a steady source of low-dose rate radiation that is primarily responsible for stochastic effects, such as cancer, and can effect the response of the central nervous system. Nuclear interactions of these components with the Martian atmosphere produces substantial flux of neutrons with high radio biological effectiveness. The uncertainty in the knowledge of many fragmentation cross sections and their energy dependence required by radiation transport codes, uncertainties in the ambient radiation environment, and knowledge of the Martian atmosphere, lead to large enough uncertainties in the knowledge of calculated radiation dose in free space (cruise phase) in Martian orbit. Direct measurements of radiation levels; of the relative contributions of protons, neutrons, and heavy ions; and of Martian atmospheric characteristics are thus prerequisites for any human mission. The orbiter spectrometer will measure the energy spectra of SEP events from 15 to 500 MeV/n, and when the results are combined with data from other space-based instruments, such as the Advanced Composition Explorer (ACE), would provide accurate GCR spectra also.

5.1 Orbiter Instrumentation

MARIE consists of the backplane, the central processing unit (CPU), power supply, and onboard data storage. The orbiter instrument contains an energetic particle spectrometer that can measure the elemental energy spectra of charged particles over an energy range of 15–450 MeV/n. The spectrometer is mounted on the science deck and has an angular acceptance of 50°. As the spacecraft orbits Mars, the axis of this field of view sweeps a cone of directions on the sky. During each orbit, the angle between the axis of the spectrometer's field of view and the mean interplanetary field direction varies from 90° to 180°.

Figure 5-1 shows a schematic of the proposed spectrometer. It consists of a set of solid-state detectors and a high–refractive-index Cerenkov detector. The basic telescope geometry is defined by two ion-implanted silicon solid state detectors, A1 and A2, that are operated near 160 V. In between A1 and A2 are two position-sensitive detectors (PSD), each with a wire grid, to define the incident direction of charged particle. These are followed by a set of lithium-drifted silicon solid-state detectors (B1, B2, B3, and B4), and a Schot-glass Cerenkov (C) detector. The telescope is built like a personal computer. Each detector has its own card, with all of the electronics associated with the detector on it, including a 12-bit analog-to-digital converter (ADC), and field-programmable gate array (FPGA). The main power supply is a nominal 28-V (16–32) DC Interpoint unit. There is an 80-MB flash memory for data storage. The CPU board has an Intel microprocessor, and data communication hardware for transferring data either in real time or delayed transmission from the storage memory. The instrument is a dE/dx × E telescope for stopping particles and dE/dx × C telescope for penetrating particles. We will also record the following coincident rates: A1A2, A1A2B1, A1A2B1B2, A1A2B1B2B3, A1A2B1B2B3B4, and A1A2B1B2B3B4C. The basic trigger is the A1A2 coincidence, which requires a proton with energy >15 MeV. Following such a trigger, all of the detectors are read out.

Data from the spectrometer are analyzed as follows. The data are divided into three energy regimes: (1) particles that stop in any detector from A2 to B4, (2) particles that go through B4 but do not give a Cerenkov signal, and (3) particles that give a Cerenkov signal. The angular information from the PSD would ensure that the particle falls in the right geometry.

Case 1 (particles that stop in any detector from A2 to B4): If the range energy relation for protons in silicon is expressed as a power law in energy with index, n, $R = KE^n$; ΔE is the energy loss in the thin detectors (A1 or A2); and E is the total energy deposited by the stopping particle, then

$$\Delta E \times (E - \Delta E) \propto Z^2 M^{n-1}$$

where Z is the charge multiple and M the mass of the incident particle, quantities that are element- and isotope-specific.

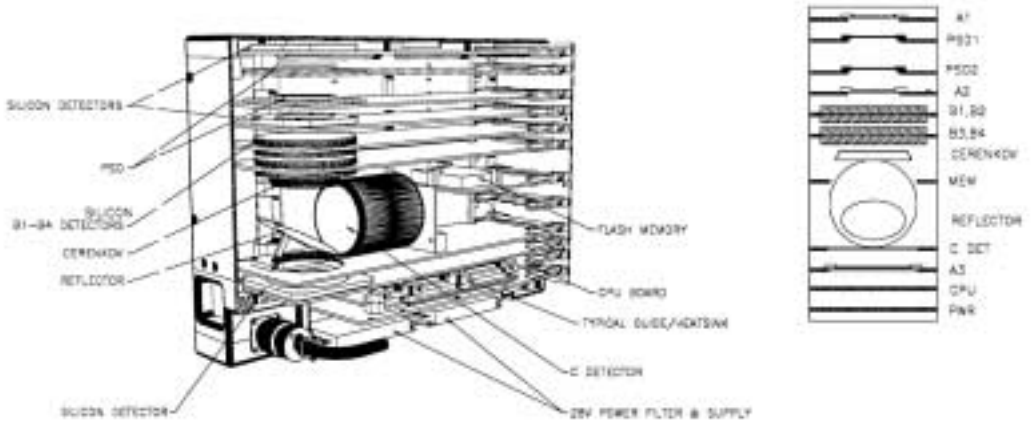

Figure 5-1. Schematic of Orbiter Spectrometer

Thus, for each isotope, we have a separate hyperbolic curve, and the charge, the mass, and the energy of the stopping particle can be determined. Figure 5-2 shows a plot of the energy loss in A1 versus the energy loss in A2 for protons and helium nuclei from the flight of a similar telescope (with no PSDs, but an anti-coincidence counter).

Case 2: In this case we already know that the particle energy is greater than the energy required to penetrate all of the detectors, but the energy is below the Cerenkov threshold of about 180 MeV/n. In this case, we use the measurements of energy loss in each of the six silicon detectors and compare it with values calculated for a given energy. The energy is varied to find the best fit by minimizing the merit function:

$$\chi^2 (E) = \sum [\Delta E_i^{cal} - \Delta E_i^{obs}]^2$$

where i (=1,6) is the index for the detector and *cal* and *obs* refer to the calculated and observed energy losses.

Case 3: In this case, the light emitted in the Cerenkov detector, C, is given by:

$$C = k Z^2 (1 - \beta_o^2/\beta^2).$$

where β_o is the threshold velocity (=1/real part of index of refraction), and β is the particle velocity and the energy loss, ΔE, is

$$\Delta E \propto Z^2/\beta^2$$

These two equations can be solved to obtain the charge and velocity (energy per nucleon). Using Schot glass we can cover the energy range from about 180 MeV/n to 500 MeV/n.

Thus, this technique can cover the entire range from the minimum energy required to form the A1A2 coincidence, to the energy where the Cerenkov response saturates. In addition, we can construct a good integral spectra of SEP events, independently, from various coincident rates. An additional advantage of such an instrument is that using the energy loss in A1 and A2 and the angle of the incident particle, a true linear energy transfer (LET) spectrum of particles can be determined.

The AΩ of the proposed instrument is not large enough for the study of high Z (>2) GCR particles. We plan to use our measurements of protons and helium GCR particles and correlate them with measurements from the ACE instrument (at L1) to obtain accurate GCR spectra in the Martian orbit.

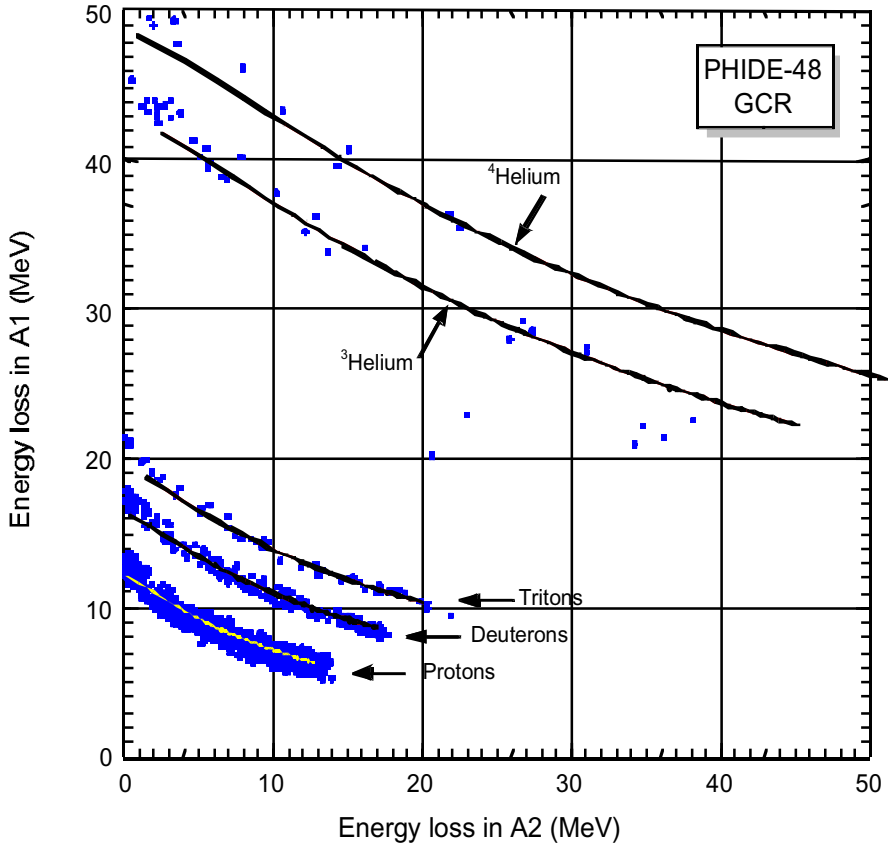

Figure 5-2. Energy Loss in A1 Detectors vs. Energy Loss in A2 Detectors

These GCR spectra (which arrive isotropically) and the complete descriptions of the SEP events measured on the orbiter are the input spectral functions to radiation transport models to predict the flux, dose, and LET spectra on the Martian surface. Because the arrival direction distribution of SEPs has been measured, proper account can be taken of the shielding presented by the Martian atmosphere and the solid planet to different arrival directions. Predicted fluxes, doses, and LET spectra will provide key radiation information for both the cruise and landed phase of future manned interplanetary missions.

6.0 ADDITIONAL INFORMATION

6.1 Web Sites

Mars Exploration Program	http://mars.jpl.nasa.gov/
2001 Mars Odyssey	http://mars.jpl.nasa.gov/odyssey/
GRS	http://grs8.lpl.arizona.edu/main.jsp
MARIE	http://mars.jpl.nasa.gov/odyssey/technology/marie.html
THEMIS	http://themis.asu.edu/

7.0 REFERENCES

Arvidson, R. and S. Slavney. 2000. *Mars Surveyor Program Data Management Plan*, Rev. 1.11.

Bard, S. 1984. Advanced passive radiator for spaceborne cryogenic cooling. *Journal of Spacecraft and Rockets* 21:150–155.

Bard, S., J. Stein, and S. W. Patrick. 1982. Advanced Radiative Cooler with Angled Shields. In *Spacecraft Radiative Transfer and Temperature Control*, edited by T. E. Horton. Volume 83. American Institute of Aeronautics and Astronautics.

Bertsch, D. L., C. E. Fichtel, and J. I. Trombka. 1988. Instrumentation for gamma-ray astronomy. *Space Science Review* 48:113–168.

Boynton, W. V., J. I. Trombka, W. C. Feldman, J. R. Arnold, P. A. J. Englert, A. E. Metzger, R. C. Reedy, S. W. Squyres, H. Waenke, S. H. Bailey, J. Brueckner, J. L. Callas, D. M. Drake, P. Duke, L. G. Evans, E. L. Haines, F. C. McCloskey, H. Mills, C. Shinohara, and R. Starr. 1992. Science applications of the Mars Observer gamma ray spectrometer. *Journal of Geophysical Research* 97(5):7681–7698.

Brückner, J., H. Wänke, and R. C. Reedy. 1987. Neutron-induced gamma-ray spectroscopy: Simulations for chemical mapping of planetary surfaces. Proceedings of the 17th Lunar and Planetary Science Conference, Part 2. *Journal of Geophysical Research* 92:E603–E616.

Brückner, J., M. Koerfer, H. Wänke, A. N. F. Schroeder, D. Filges, P. Dragovitsch, P. A. J. Englert, A. J. Peter, R. Starr, J. I. Trombka, I. Taylor, D. Drake, and E. R. Shunk. 1990. Radiation damage in germanium detectors: Implications for the gamma-ray spectrometer of the Mars Observer spacecraft. *Proceedings of the 21st Lunar and Planetary Science Conference*, 137–138.

Brückner, J., M. Koerfer, H. Wänke, A. N. F. Schroeder, D. Filges, P. Dragovitsch, P. A. J. Englert, R. Starr, J. I. Trombka, I. Taylor, D. M. Drake, and E. R. Shunk. 1991. Proton-induced radiation damage in germanium detectors. *IEEE Transactions on Nuclear Science*. 38(2):209–217.

Dagge, G., P. Dragovitsch, D. Filges, and J. Brückner. 1991. Monte Carlo simulation of Martian gamma-ray spectra induced by galactic cosmic rays. *Proceedings of the 21st Lunar and Planetary Science Conference*, 425–435.

Drake, D. M., W. C. Feldman, and B. M. Jakosky. 1988. Martian neutron leakage spectra. *Journal of Geophysical Research* 93:6353–6368.

Evans, L. G., and S. W. Squyres. 1987. Investigation of Martian H_2O and CO_2 via orbital gamma ray spectroscopy. *Journal of Geophysical Research* 92:9153–9167.

Evans, L. G., R. C. Reedy, and J. I. Trombka. 1993. Introduction to Planetary Remote-Sensing Gamma-Ray Spectroscopy. In *Remote Geochemical Analysis*, edited by C. M. Pieters and P. A. J. Englert. Houston, Texas: Lunar and Planetary Institute.

Feldman, W. C., and D. M. Drake. 1986. A Doppler filter technique to measure the hydrogen content off planetary surfaces. *Nuclear Instruments and Methods in Physics Research, Section A: Accelerators, Spectrometers, Detectors and Associated Equipment*. 245:182–190.

Feldman, W. C., W. V. Boynton, and D. M. Drake. 1993. Planetary Neutron Spectroscopy from Orbit. In *Remote Geochemical Analysis*, edited by C. M. Pieters and P. A. J. Englert. Houston, Texas: Lunar and Planetary Institute.

Kruse, H. 1979. Spectra processing with computer graphics. In *Computers in Activation Analysis and Gamma-Ray Spectroscopy*, *Proceedings of the American Nuclear Society Topical Conference*, edited by B. S. Carpenter, M. D. D'Agostino, and H. P. Yull. pp. 76–84, U.S. Dept. Of Energy, Washington, D.C.

Yadav, J. S., J. Brückner, and J. R. Arnold. 1989. Weak peak problem in high resolution gamma-ray spectroscopy. *Nuclear Instruments and Methods in Physics Research, Section A: Accelerators, Spectrometers, Detectors and Associated Equipment* A277:591–598.

8.0 ACRONYMS

A/D	analog-to-digital
AC/N	anticoincidence shield/neutron detector
ACE	advanced composition explorer
ADC	analog-to-digital converter
CCD	charge coupled device
CCSDS	Consultative Committee for Space Data Systems
CD-WO	compact disk-write only
CEA	central electronics assembly
CPU	central processing unit
DC	direct current
DSN	Deep Space Network
DVD	digital video disk
EDR	experiment data records
ET	ephemeris time
FOV	field of view
FPGA	field programmable gate array
FSE	front stage electronics
FWHM	full-width at half-maximum
GCR	galactic cosmic rays
GMT	Greenwich Mean Time
GRS	gamma ray spectrometer
GSD	ground sampling distance
GSH	gamma sensor head
HEDS	Human Exploration and Development of Space
HEND	high-energy neutron detector
HPGe	high-purity germanium
HZE	high energy and charge
IAU	International Astronomical Union
IFOV	instantaneous field of view
IR	infrared
IRDA	infrared detective assembly
IRIS	infrared imaging subsystem
IRS	infrared subsystem
JPL	Jet Propulsion Laboratory
LET	linear energy transfer
LMA	Lockheed Martin Astronautics, Inc.
LMST	local mean solar time
LTST	local true solar time
MARIE	Martian Radiation Environment Experiment
Mars 2001	Mars Surveyor Program 2001 Mars Odyssey Mission
MGS	Mars Global Surveyor
MOI	Mars orbit insertion
MSP	Mars Surveyor Program
MTF	modulation transfer function
NAIF	Navigation and Ancillary Information Facility
NASA	National Aeronautics and Space Administration
NAV	navigation team
NE$\Delta\varepsilon$	noise equivalent delta emissivity
NS	neutron spectrometer
NSSDC	National Space Science Data Center
OSS	Office of Space Science

PDS	planetary data system
PHA	pulse height analyzers
PI	principal investigator
PIP	proposal information package
PMT	photomultiplier tube
PSD	position sensitive detector
PSG	project science group
PST	planning and sequencing team
SCT	spacecraft team
SDVT	science data validation team
SEP	solar energetic particle
SIS	Software Interface Specification
SNR	signal-to-noise ratio
sol	one Martian day
SOT	science operations team
SPICE	Spacecraft Planet Instrument Camera-Matrix Events
TDI	time delay integration
TES	Thermal Emission Spectrometer
THEMIS	Thermal Emission Imaging System
TMOD	Telecommunications and Mission Operations Directorate
VIS	visible imaging subsystem

Chemical Elements

Al	aluminum
As	arsenic
C	carbon
Ca	calcium
Cd	cadmium
Cl	chlorine
Cm	curium
Co	cobalt
Cr	chromium
Cu	copper
Fe	iron
Ga	gallium
Gd	gadolinium
Ge	germanium
H	hydrogen
Hg	mercury
In	indium
K	potassium
Li	lithium
Mg	magnesium
Mn	manganese
N	nitrogen
Na	sodium
Ni	nickel
O	oxygen
P	phosphorus
Pb	lead
Rh	rhodium
S	sulphur
Si	silicon

Th	thorium
Ti	titanium
U	uranium

Appendix A

Caveat: Although the plans for the Mars 2001 data archive and generation given in this appendix are preliminary and not officially approved, we have included this information as an aid to potential proposers.

2001 Mars Odyssey Orbiter

ARCHIVE GENERATION, VALIDATION, AND TRANSFER PLAN

DRAFT

November 3, 2000/updated 03/01/01

2001 Mars Odyssey Orbiter

ARCHIVE GENERATION, VALIDATION, AND TRANSFER PLAN

DRAFT

Prepared by:

_____
Raymond E. Arvidson
Interdisciplinary Scientist for Data and Archives, Mars Exploration Program

Approved by:

_____
Gautam Badhwar
Principal Investigator, MARIE

_____
R. Stephen Saunders
Project Scientist

_____
William Boynton
Principal Investigator, GRS

_____
Scott Hubbard
Mars Exploration Program Director

_____
Philip Christensen
Principal Investigator, THEMIS

_____
Elaine Dobinson
Project Manager, Planetary Data System

_____
Michael Meyer
Program Scientist

_____
Joseph H. King
Director, NSSDC

November 3, 2000/
updated 03/01/01

DOCUMENT CHANGE LOG

Date	Description	Sections affected
9/24/99	Initial draft	All
7/24/00	Removed references to 2001 Lander	All
8/25/00	Corrected dates of instrument operation based on timeline in Mission Plan	5.3, Table 6
10/17/00	Remove Tom Thorpe from signature page and added Scott Hubbard	Signature page
10/17/00	Added statement that SPICE kernels are generated by Project and archived by NAIF	3.0
10/17/00	Removed Figure 2, Flow of archive volume generation, validation and transfer (TBD)	Figure 2
11/3/00	Removed Figure 1, Mission Timeline (TBD)	Figure 1
11/3/00	Revised to include new paradigm for electronic data distribution	2, 3, 4, 5
11/3/00	Changed Mars Surveyor 2001 to 2001 Mars Odyssey Orbiter	All

TBD ITEMS

Section	Description
1.4 Applicable Documents and Constraints	Complete references for several documents are TBD.
Table 3-4. Mars Odyssey Orbiter Standard and Special Products	Parts of the table are TBD.
Header on every page	This document needs Project and JPL document numbers.

CONTENTS

1. INTRODUCTION A-5
1.1 Purpose A-5
1.2 Scope A-5
1.3 Contents A-5
1.4 Applicable Documents and Constraints A-5
2. OVERVIEW OF MARS ODYSSEY ORBITER MISSION A-6
2.1 Mission Overview A-6
2.2 Ground Data System A-7
3. OVERVIEW OF ARCHIVING FUNCTIONS A-9
3.1 Generation of Archives A-9
3.2 Validation and Delivery of Archives to the Planetary Data System A-9
3.3 Distribution of Data Products A-10
3.4 Permanent Storage and Backups A-10
4. ROLES AND RESPONSIBILITIES A-16
4.1 Mars Odyssey Project A-16
4.2 Planetary Data System A-16
4.3 National Space Science Data Center A-16
5. ARCHIVE GENERATION, VALIDATION, AND RELEASE SCHEDULES A-16
5.1 Integrated Archives A-16
5.2 Delivery Schedule A-17

TABLES

Table 2-1. Mars Odyssey Orbiter Payload A-8
Table 3-1. Components of Mars Odyssey Orbiter Archives A-10
Table 3-2. Mars Odyssey Orbiter Archive Component Suppliers A-12
Table 3-3. Definitions of Processing Levels for Science Data Sets A-14
Table 3-4. Mars Odyssey Orbiter Standard and Special Data Products A-15
Table 5-1. Mars Odyssey Orbiter Archive Delivery Schedule A-18

1. INTRODUCTION

1.1 Purpose

The purpose of this document is to provide a plan for generation, validation, and transfer to the Planetary Data System (PDS) of 2001 Mars Odyssey Orbiter Mission archives containing raw and reduced data, documentation, and algorithms/software. Release of data to the public is delineated in a separate Public Information Plan.

1.2 Scope

The plan covers archiving of raw and reduced data sets and related information to be acquired or derived during the Mars Odyssey Orbiter Mission.

Specific aspects addressed in this plan are:

1. Generation of high-level mission, spacecraft and instrument documentation, instrument calibration reports, algorithms, and documentation of software used to produce reduced data records (RDRs).
2. Reduction of science packet data to experiment data records (EDRs) and RDRs, including generation of data sets expressed in geophysical units, with associated documentation that determines when and where the data were acquired and for what purpose.
3. Generation of ancillary dat archives in the NASA "SPICE" format, for use with allied SPICE Toolkit software freely available from the Navigation and Ancillary Information Facility (NAIF) at JPL.
4. Generation and validation of PDS compliant archives containing Odyssey EDRs and RDRs, software, algorithms, documentation, and ancillary information.
5. Delivery to the community of validated Odyssey archives through the PDS.
6. Generation of deep archive volumes for permanent storage at the National Space Science Data Center (NSSDC).

1.3 Contents

This plan begins with a summary of Mars Odyssey mission phases, expected data volumes, and an overview of the ground data system. This section is followed by a description of the roles and responsibilities for organizations and personnel associated with generation, validation, and distribution of Odyssey archives that are compliant with PDS standards. The document ends with specific plans for each archive function: generation, validation, transfer, and distribution.

1.4 Applicable Documents and Constraints

The Archive Plan flows from and is responsive to the documents listed below.

1. Mars Exploration Program Data Management Plan, R. Arvidson and S. Slavney, Rev. 1.11, 2000.
2. Project Plan (reference TBD).
3. Mars Odyssey Orbiter Mission Plan, Rev. A, JPL D-16303, May 1999.
4. Investigation Description and Science Requirements Document (reference TBD).
5. Project Data Management Plan (reference TBD).

6. Mission Operations (reference TBD).

The plan is consistent with the principles delineated in the following National Academy of Sciences reports:

7. Data Management and Computation, Volume 1, Issues and Recommendations, 1982, National Academy Press, 167 p.
8. Issues and Recommendations Associated with Distributed Computation and Data Management Systems for the Space Sciences, 1986, National Academy Press, 111p.

The plan is also consistent with the following Planetary Data System documents:

9. Planetary Data System Data Preparation Workbook, February 1, 1995, Version 3.1, JPL D-7669, Part 1.
10. Planetary Data System Data Standards Reference, June 1, 1999, Version 3.3, JPL D-7669, Part 2.

Finally, the plan is meant to be consistent with the contracts negotiated between the Mars Odyssey Project and each Principal Investigator (PI) in which EDRs and RDRs and associated documentation are explicitly defined as deliverable products.

2. OVERVIEW OF MARS ODYSSEY ORBITER MISSION

2.1 Payload and Mission

The Odyssey Orbiter will carry three science instruments, the Thermal Emission Imaging System (THEMIS), the Gamma Ray Spectrometer (GRS), and the Martian Radiation Environment Experiment (MARIE). THEMIS will map the mineralogy and morphology of the martian surface using multispectral imaging in the visible and thermal infrared. GRS will map the elemental composition of the surface. GRS also includes a suite of neutron spectrometers and a High Energy Neutron Spectrometer (HEND) to map the abundance of hydrogen in the shallow subsurface. Depth of the seasonal carbon dioxide polar caps will also be inferred from data collected by the neutron spectrometer subsystem on GRS. HEND data will be used to define a time series of gamma ray bursts and charged particle events. MARIE will characterize the near-space radiation environment. MARIE is an instrument provided by the Human Exploration and Development of Space Program, whereas THEMIS and GRS are provided through the Office of Space Science. Table 2-1 summarizes the Odyssey Orbiter payload.

The Mars Odyssey Orbiter is scheduled for launch in April 2001 and will arrive at Mars in October 2001. The Orbiter will use aerobraking to be placed into a 400 km circular orbit about 45 days after arrival. The nominal science mission for the Mars Odyssey Orbiter extends for 917 Earth days after the spacecraft has achieved a near-circular orbit in December 2001. MARIE will acquire data continuously throughout the science mission. On the other hand, THEMIS and GRS have conflicting observation requirements. Signal to noise issues require THEMIS observations to occur before 5:00 pm local true solar time. The initial mapping orbit is designed to achieve a LTST of 4:13 pm, consistent with requirements for thermal imaging. However, the GRS requires a beta angle of less than –57.5 degrees, which is violated during the initial mapping orbit. To meet both requirements the spacecraft orbital node precession rate is controlled so that appropriate observing periods are reached during the mapping mission for both payloads. GRS will begin acquiring data approximately 120 days into the science mission and will continue until the end of the science mission in June 2004. THEMIS will have two periods of data acquisition, the first from December 2001 through October 2002, and the second from September 2003 to the end of the mission.

During the mission approximately 942 gigabits of data will be returned from THEMIS, 68 gigabits from GRS, and 2.8 gigabits from MARIE for a total volume of science telemetry of 1012.8 gigabits or approximately 1 terabit of data.

2.2 Ground Data System

Principal Investigators are responsible for retrieving science packets (science telemetry), SPICE files, and other relevant information from the appropriate project data bases and transferring the files to their respective home institutions, using electronic transfer. Principal Investigators will generate EDRs and RDRs at their home institutions and will make these products available to Co-Investigators and other personnel, using the data use policies outlined in the Mars Exploration Program Data Management Plan. Once EDR and RDR data products have been validated and released to PDS as archives, the data and associated information will be made available to the research, education, and public communities.

Table 2-1. Mars Odyssey Orbiter Payload

THEMIS (Thermal Emission Imaging System	THEMIS data sets will consist of 9 band thermal infrared (6.3 to 15.5 micrometers) images with 100 m/pixel and 5 band visible-reflected infrared (0.425-0.950 micrometers) images with 20 m/pixel. The data sets will be used to determine the mineralogy and thermophysical properties of Mars, to map the surface morphology, and to search for hydrothermal systems using pre-dawn observations.	P. Christensen, Arizona State University
GRS (Gamma-Ray Spectrometer)	GRS derived data sets will consist of a suite of global maps depicting elemental ratios and abundances with an accuracy of 10% or better and a spatial resolution of about 300 km. The prime data products from the NS and HEND will be global maps depicting hydrogen (with depth of water inferred) and polar CO_2 ice abundances. An additional HEND data product will consist of time series of gamma ray and particle fluxes from non-martian sources.	W. Boynton, University of Arizona
MARIE (Martian Radiation Environment Experiment)	MARIE data sets will consist of H and He energy spectra associated with solar energetic events and galactic cosmic rays from approximately 15 MeV/n to 500 MeV/n.	G. Badhwar, Johnson Space Center

3. OVERVIEW OF ARCHIVING FUNCTIONS

Standard products form the core of the archives to be produced by Odyssey and released to the PDS for distribution to the science community and others. Standard products are well-defined, systematically generated data products, i.e., EDRs and RDRs. These products and associated supporting information (e.g. documentation, index tables) will be validated and delivered to the PDS at regular intervals. Table 3-1 lists the elements that comprise the Odyssey archives, and Table 3-2 lists the suppliers of data and information for the archives. Table 3-3 shows the standard processing levels defined for science data. Standard products for each instrument are listed in Table 3-4.

In the following section we discuss the processes and schedules for generation and validation of standard products and archives, delivery to the PDS, and distribution to the science and other communities.

3.1 Generation of Archives

Instrument science packets, spacecraft engineering packets, other engineering information and data, and SPICE kernels will be generated by Mars Odyssey Data Administration and archived by NAIF. Principal Investigators will access instrument science and engineering packets, and ancillary information such as spacecraft position and orientation in SPICE file format, from the project database. These will be used to generate NASA Level 1A Experiment Data Records (EDR) and higher-level derived products (see Table 3-3). These data products will form the Mars Odyssey science data archives, along with supporting materials such as documentation, index tables, calibration files, and algorithms and/or software. The archives will be assembled under Principal Investigator auspices with guidance and assistance as needed from the Mars Odyssey Interdisciplinary Scientist for Data and Archives and the Mars Odyssey Data and Archives Working Group (DAWG). The DAWG will also help generate plans for these archives and provide oversight during the archiving phase of the mission.

3.2 Validation and Delivery of Archives to the Planetary Data System

The Planetary Data System requires that science archives be validated both for scientific integrity and for compliance with PDS standards. Validation will be done at several points along the path from receipt of raw packets to delivery of standard products, by a combination of mission and PDS personnel. Broad oversight of the validation work will be accomplished by the Science Data Validation Team (SDVT), a multi-mission team that ensures that all Mars Exploration Program projects are maintaining archiving schedules. The DAWG will work on a detailed level to ensure that validation steps are accomplished.

Validation of standard products and associated information will be done by the instrument teams as an integral part of their data analysis work. Standard products will then be assembled with supporting materials such as labels, index tables, documentation and software to form archives.

An important step is the validation of standard product archives before delivery to the PDS. The first archive delivery from an instrument will undergo a formal PDS peer review with participation by mission personnel, PDS personnel, and invited reviewers from the science community, under DAWG auspices. The archives will be examined for integrity of scientific content, compliance with the applicable Data Product Software Interface Specification (SIS) and Archive SIS, and compliance with PDS standards. Often a peer review will result in requests for changes or additions to the supporting material in the archive ("liens"). The liens will be resolved before the archive can be

accepted by PDS. Subsequent deliveries of archives throughout the mission are not required to undergo another peer review, as long as they do not vary substantially from the first delivery. They are, however, required to pass a validation check for PDS compliance. If minor errors are found, they may simply be documented in an errata file that accompanies the archive. Major errors will be corrected before the archive is accepted by PDS. When an archive has passed peer review and the PDS validation check, it will then be considered to be released, or "delivered", to the PDS.

3.3 Distribution of Data Products

The Mars Odyssey Project is responsible for making data products available to its own personnel. The PDS is responsible for making data products available to the rest of the science community and to the public.

Archives from previous missions have often been distributed to the science community on a set of physical media (e.g. CD-ROMs). The large volume of data expected from Mars Odyssey makes this form of distribution expensive and impractical. Instead, distribution will be accomplished chiefly by Internet access in ways that take advantage of the capabilities and expertise associated with Principal Investigator home institution systems. Specifically, the MARIE archives will be transferred to the PDS Geosciences Node at Washington University for on-line access once the archives have been validated and released. GRS RDRs will likewise be transferred to the Geosciences Node for online access. In addition, the University of Arizona GRS facility will retain EDRs and become a Geosciences Data Node, processing data on demand for special purposes as required by the research community. The special products will be made available to the entire community through the Geosciences Node. For THEMIS, because of the expertise and extensive facilities located at the Arizona State University THEMIS facility, all archives will remain at the THEMIS site. The PDS Geosciences and Imaging Nodes will access the relevant EDRs and RDRs online, package the data based on user requests, and provide the community with custom-generated orders. The Arizona University site thus also becomes a PDS Data Node. It is the intent to fill as many orders as possible using online systems. The PDS is also prepared to generate hard copy volumes (primarily DVDs) as needed.

3.4 Permanent Storage and Backups

The PDS is responsible for maintaining copies of its science archives on permanent physical media, and for delivering copies of science archives to the National Space Science Data Center (NSSDC). As archives are released to the PDS, the Geosciences Node (or its GRS and THEMIS Data Nodes) will generate at least two copies on appropriate physical media for long-term storage by PDS and NSSDC.

During the six-month validation period before delivery, and the interval following delivery during which the Geosciences Node is writing the archives to physical media, the data products will exist as online archives only. To reduce the risk of data loss, the Mars Odyssey Project is responsible for conducting periodic backups or otherwise maintaining redundant copies of online archives until they are permanently stored with PDS.

Table 3-1. Components of Mars Odyssey Orbiter Archives

SPICE Archives	• SPICE Kernel Software Interface Specification Documents

	• SPICE Kernels • SPICE Toolkit Software
Science Data Archives	• High-level mission, spacecraft, instrument, and data set descriptions for the PDS Catalog • Data Product Software Interface Specification (SIS) Documents • Archive Volume Software Interface Specification Documents • Processing Descriptions, Algorithms, and Software (to use in understanding reduced data product generation) • Instrument Calibration Reports and associated data needed to understand level 1 product generation • Standard Data Products with PDS Labels (Level 0 Experiment Data Records and higher order products)
Engineering Data Archives	• Archive Volume Software Interface Specification Document • Data Product Software Interface Specification Documents • Science Data Packets • Engineering Data Products • Other products as appropriate

Table 3-2. Mars Odyssey Orbiter Archive Component Suppliers

NAIF Team	• Consolidated SPK files (ephemerides of spacecraft and target bodies) • Planetary constants (PcK) • Selected Instrument geometry (IK) • Reference frame specifications (FK) • Orientation of spacecraft, HGA and solar array (CK) • As-run sequence of events in database form (part of EK) • Experimenter's Notebook (part of EK) • Spacecraft clock coefficients (SCLK) • Tabulation of leapseconds (LSK) • Tabulation of orbit number boundaries (ORBNUM)
Science Operations Team	• Planetary Data System high-level catalog templates • E Kernel contributions---instrument specific • Experiment Data Records including labels and ancillary information • Reduced Data Records including labels and ancillary information • Processing algorithms and software to go from level 0 to higher level products, typically level 1 • Instrument calibration reports and associated data
Data Administration	• Science packet data • Engineering packet data • Monitor data • Engineering data archive files
Spacecraft Team	• Spacecraft Status Report • Mission Controllers Real-Time Operations Log
Navigation Team	• SP Kernels

Mission Planning and Sequencing Team	• Predicted Events File as input to the E Kernel • Sequence of Events File as input to the E Kernel
All Teams	• Data Product and Archive Volume Software Interface Specification documents • Contributions to Experimenter's Notebook

Table 3-3. Definitions of Processing Levels for Science Data Sets

NASA	CODMAC	Description
Packet data	Raw - Level 1	Telemetry data stream as received at the ground station, with science and engineering data embedded.
Level 0	Edited - Level 2	Instrument science data (e.g., raw voltages, counts) at full resolution, time ordered, with duplicates and transmission errors removed.
Level 1A	Calibrated - Level 3	Level 0 data that have been located in space and may have been transformed (e.g., calibrated, rearranged) in a reversible manner and packaged with needed ancillary and auxiliary data (e.g., radiances with the calibration equations applied).
Level 1B	Resampled - Level 4	Irreversibly transformed (e.g., resampled, remapped, calibrated) values of the instrument measurements (e.g., radiances, magnetic field strength).
Level 1C	Derived - Level 5	Level 1A or 1B data that have been resampled and mapped onto uniform space-time grids. The data are calibrated (i.e., radiometrically corrected) and may have additional corrections applied (e.g., terrain correction).
Level 2	Derived - Level 5	Geophysical parameters, generally derived from Level 1 data, and located in space and time commensurate with instrument location, pointing, and sampling.
Level 3	Derived - Level 5	Geophysical parameters mapped onto uniform space-time grids.

Table 3-4. Mars Odyssey Orbiter Standard and Special Data Products

	Product	Description	Data Volume (Gbits)
MARIE	MARIE-EDR	Raw time series of counts and radiation levels for various detectors	TBD
	MARIE-RDR	Time series of radiation levels reduced to geophysical units	TBD
THEMIS	THM-VISEDR	Image cube of visible bands	1000.0
	THM-IREDR	Image cube of infrared bands	1000.0
	THM-VISRDR	Visible-band image cubes in radiance units	1000.0
	THM-IRRDR	Infrared-band image cubes in radiance units	1000.0
GRS	GRS-EDR	Raw spectra	TBD
	GRS-RDR	Maps of element ratios and/or concentrations	TBD
	GRB-EDR	Gamma ray burst and charged particle events as time series of counts	TBD
	GRB-RDR	Gamma ray burst and charged particle events as time series of fluxes	TBD
	NS-EDR	Raw spectra	TBD
	NS-RDR	Maps of hydrogen concentrations and carbon dioxide ice thickness	TBD
	HEND-EDR	Raw spectra	TBD
	HEND-RDR	Maps of hydrogen concentrations	TBD
SPICE	SPK	SPK kernels	TBD
	PcK	PcK kernels for times of interest	TBD
	IK	I kernels for instruments	TBD
	CK	C kernels for spacecraft rotations	TBD
	EK	E kernels delineating sequences and Experimenter's Notebooks depicting events	TBD
		Total data volume	4000+

4. ROLES AND RESPONSIBILITIES

In this section the roles and responsibilities for personnel and organizations involved in Mars Odyssey archive generation, validation, delivery, and distribution are summarized.

4.1 Mars Odyssey Project

The Project Scientist and the Project Science Group, through the Data and Archives Working Group (DAWG), provide an oversight function for implementation of the Archive Generation, Validation, and Transfer Plan. The Mars Exploration Program Interdisciplinary Scientist for Data and Archives will advise the Project with regard to archiving and will work with Mars Odyssey and the PDS to help ensure that detailed plans are in place for generation of Planetary Data System-compatible products and associated documentation, and that archive volumes are generated, validated, and transferred to the Planetary Data System.

The Mars Odyssey project will archive engineering and science packets from spacecraft instruments, DSN monitor data, and SPICE files. Principal Investigators will generate archive volumes containing EDRs and RDRs, documentation, algorithms or software to generate at least Levels products, and other supporting materials. Each data provider is responsible for publishing Data Product Software Interface Specification (SIS) documents that describe in detail the format and content of the data products, along with an Archive SIS. SISs may be included in the archives as part of the documentation.

The Mars Exploration Program Science Data Validation Team (SDVT) will be responsible for providing an oversight function that keeps archive generation, validation, and delivery on schedule.

4.2 Planetary Data System

The PDS is the designated point of contact for Mars Odyssey on archive-related issues. The PDS is also the interface between Odyssey and the NSSDC.

The PDS, through the Interdisciplinary Scientist for Data and Archives and the DAWG, will work with the SDVT and other Odyssey elements to ensure that the Odyssey archives are compatible with PDS standards and formats. The PDS will provide funds for generation, distribution, and maintenance of Odyssey archive volumes for the NASA-supported science community. It may be necessary to augment the basic PDS funding line with MODA funds for the new GRS and THEMIS data nodes.

4.3 National Space Science Data Center

The National Space Science Data Center will maintain a "deep archive" of Mars Odyssey data for long-term preservation and for filling large delivery orders to the science community. The PDS will deliver copies of Mars Odyssey archive volumes to NSSDC.

5. ARCHIVE GENERATION, VALIDATION, AND RELEASE SCHEDULES

5.1 Integrated Archives

The Mars Odyssey Project will release integrated archives within six months of receipt of the last raw data included in the archives, in compliance with the Mars

Exploration Program data release policy. During the six month interval the data will be processed to standard products, validated through analyses, assembled into archives (on line), and checked for compliance with PDS standards.

5.2 Delivery Schedule

The nominal science mission for the Mars Odyssey Orbiter extends for 917 Earth days after the spacecraft has achieved a near-circular orbit in December 2001. The Orbiter instruments have different scheduled times for data acquisition. MARIE will acquire data continuously throughout the science mission. GRS will begin acquiring data 158 days into the science mission and will continue until the end of the mission in June 2004. THEMIS will have two periods of data acquisition, the first from December 2001 through October 2002, and the second from about September 2003 to the end of the mission.

In accordance with the Mars Exploration Program data release policy, a six-month period after data acquisition is allotted for product generation and validation. Therefore, the first Mars Odyssey data release will occur six months after the science mission begins, and will consist of data acquired during the first month. Thereafter, data releases will occur every three months. The second delivery will consist of data collected in months 2 and 3 of the science mission. Each of the remaining deliveries will include three months' worth of data acquired six to nine months previously. See Table 5-1 for a detailed delivery schedule.

Table 5-1. Mars Odyssey Orbiter Archive Delivery Schedule